Dear Editor, dear Reviewers,

We want to thank you for the very constructive comments that you provided following your reading of the manuscript (they testify for careful examination and knowledge of the field), and for the enhanced time that you allocated us to submit this response: it was really welcome, thank you for your understanding.

This document incudes a point-by-point response to the reviewers'comments indicating changes made in the manuscript, followed by the revised manuscript with corrections highlighted.

Point-by-point response to comments by Referee # 1:

We are deeply grateful to reviewer 1 for its thorough examination of the paper and sharp, helpful comments that encompass both the wide areas of… physics and grammar!

Response to « General Remarks »

(i) About « sharpening the focus » and « concentrating on innovations »
We completely understand your feeling. Structuring the paper in its current form was actually a long debated choice: should we prefer a sharp and short paper just focused on the added-value of the 2-layer model? Or a more comprehensive one, that would also include a never-published (and hard to dig out) exhaustive documentation of the canopy module, that would help further generations of PhD students and postdoc understand the module in its present state and build on it with loads of innovative, great ideas ? We obviously chose the second option; the choice of GMD naturally ensued, as the journal fits that purpose.
For the revised version, we stand to that choice.
However, your comment means a lot to us as the feedback of a very advanced reader. You convinced us that clear efforts had to be made to make the reader aware of the particular structure of the paper, and help him better find his way to his key interests (model documentation, or state-of-the-art developments based on physics and applied on field data).
We therefore performed the following changes (that are highlighted in the corrected version attached to this Response) :
-     Clearly state our documentation purpose in the Asbtract. (« *As a by-product of these new developments, an exhaustive description of the canopy module of the SNOWPACK model is provided, thereby filling a gap in the existing literature.")*
-     We thoroughly revised our introduction and among others, insisted on the paper's structure :

"Our contribution is hence structured in the following way:

1.   an exhaustive documentation of the new model and the canopy module it is embedded in, is proposed, for the sake of clarity and knowledge dissemination. Earlier versions of the canopy module had been only partially described in Stähli et al. (2006) and in appendix A of Musselmann et al. (2012).

2.   existing simultaneous observations of sub-canopy radiation, snow evolution and meteorological conditions from Alptal (Switzerland) are used to validate the new model and demonstrate its robustness and improvement over simpler canopy formulations and with respect to observations.

40   *3.   model validity and transferability is finally tested against observations of components of the canopy energy balance taken from a different coniferous environment (Norunda, Sweden)."*

      (ii)   The methods applied are appropriate and valid. However, concerning the related work, some additions should be included. Balance of what is presented and discussed can be improved, too.

45

      The Discussion was enhanced, especially with respect to the role of longwave radiation in the spring melt dynamics below forests. The discussion about the mass-balance and the relative importance of processes affecting it was ill-placed in the previous version and now belongs to the Discussion too.

50   We feel that the first part of your concern (« additions should be included ») has to do with the possibility of including additional simulations and comparisons to observation, as you suggest later in your detailed remarks.
      We followed your advice and tested the new canopy model at BERMS and Fraser, two sites from the SnowMIP2 project.
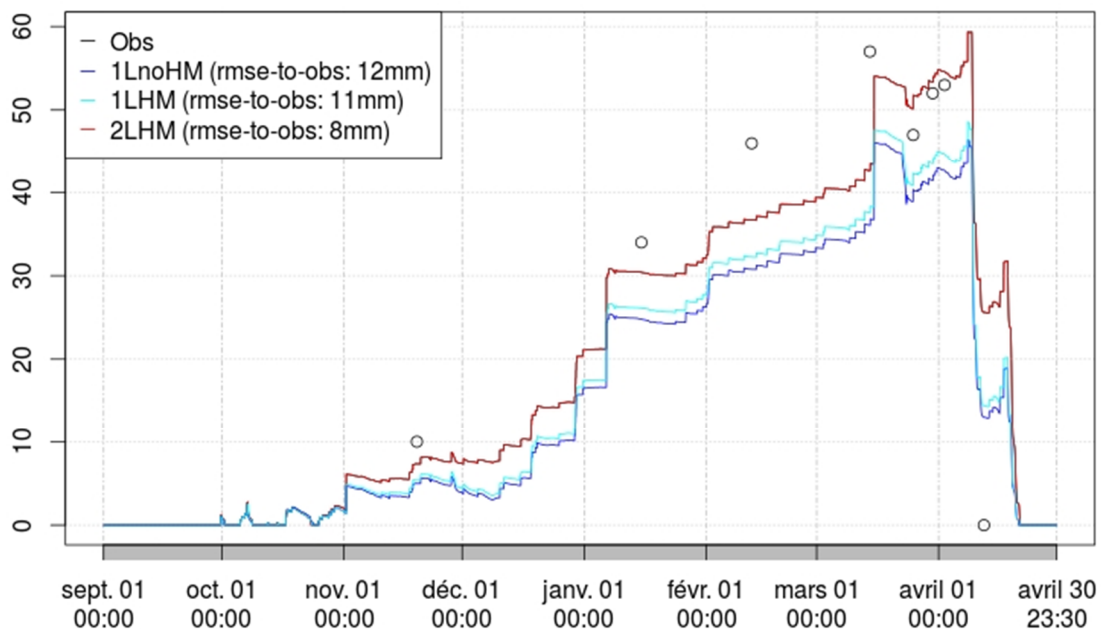
55

      Fig1. SWE observations and simulations at the BERMS site.
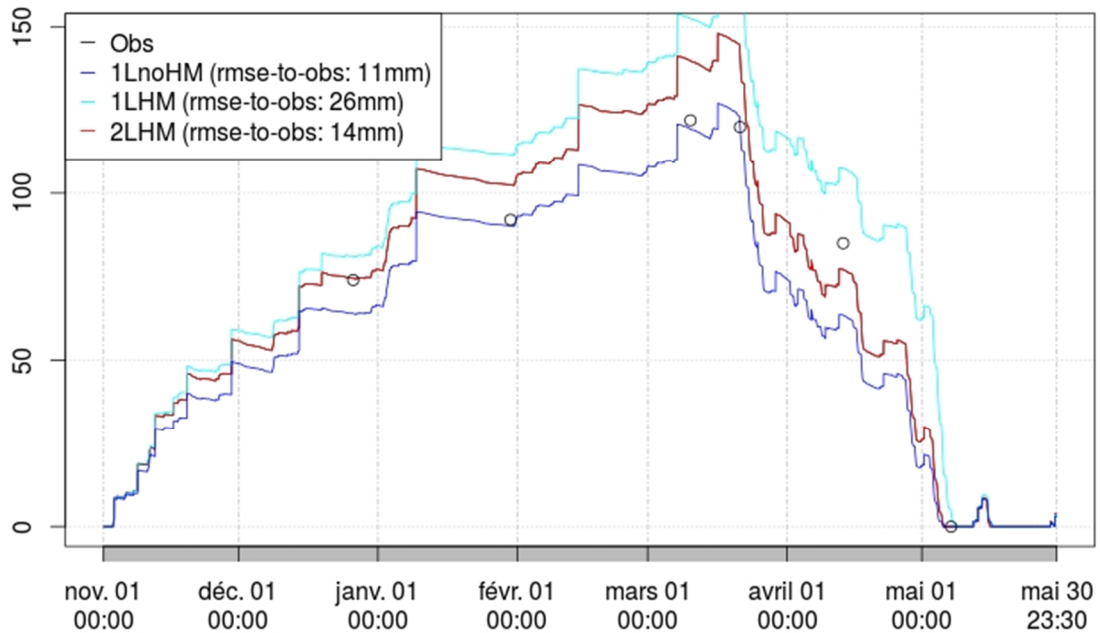
SWE (mm) at Fraser Forest, 2003-2004

Fig 2. SWE observations and simulations at the Fraser site.

For these simulations we blindly used the forest and site parameters from the SnowMIP instructions and did not calibrate the model.

These simulations confirm that the new canopy module does not deteriorate the model's ability with respect to SWE modelling, and sometimes improve it (like at BERMS).

However, none of the authors of this study is truly familiar with these sites, and we feel that this is detrimental to a proper analysis of these results. At the local Alptal site, we could use ancillary, stand-scale radiation data to calibrate some model parameters properly (like the shortwave extinction coefficient) and evaluate other aspects of the model in the best possible setup with respect to the variety of available data. Furthermore, we relied on local knowledge for improved precipitation and radiation inputs to the model.

None of this was easily feasible for the BERMS or Fraser sites.

From Rutter et al. (2009), we trust that the harsh snow-rain threshold at 2°C at Fraser limits the reliability of the precipitation fields, and hence the strength of the conclusions that could be drawn from Fig. 2. The 2LHM model outperforms other model versions at BERMS, which we are happy about, but the simulation exhibits inconsistencies in both the accumulation and ablation phases, and it is difficult to assess whether the model performance are induced by the improved parameterization or randomly by better error compensations, for interception deficiencies for instance.

We therefore chose not to elaborate on this in the corrected version of the manuscript, because an analysis as detailed as what we did at Alptal would require much data digging and site knowledge that we are currently able to put together. The use of the SnowMIP sites combined with local knowledge is though mentioned in the Discussion as a rich perspective.

(iii)   We elaborated about the structural choices made for the manuscript as an answer to (i) ; efforts were also made to sharpen the focus and make it easier to navigate through the structure depending on the reader's interests. We hope that this fulfills your demand.

(iv)   We took your helpful suggestions into account and also rephrased some ambiguous
90 paragraphs. Many thanks for this detailed help !

Response to « Remarks in Detail »

(i)   None needed

- about missing references : your bibliography suggestions have been taken into account and the
95   discussion of the SnowMIP2 case study has also been enhanced with a view of sharpening the
     precise focus of our paper, among other possible issues like mass-balance.
- About the coniferous vs deciduous, summer vs winter (snow) processes, mass balance vs energy
     balance:

100 • **Coniferous vs deciduous :**

The Reviewer is right in pointing out that the domain of validity of the model has not been specified
properly. Our new canopy module is indeed in its current form designed for **needleleaf, evergreen**
forest. We strove to explain this in the manuscript:

- The paper's title is now: « A two-layer canopy model with thermal inertia for an improved
105 snowpack energy-balance below needleleaf forest".

- We now specify in the abstract and in the text that our modelling is up to now only valid for
needleleaf, evergreen forests.

-      It is stated in the discussion that « *The two-layer formulation furthermore builds a suitable*
110 *basis for a future model adaptation to deciduous forest environments*"

• **Summer vs winter (snow) processes :**

The SNOWPACK model was originally designed for snow applications. However, as an energy-balance
model featuring a conservative soil scheme with water balance and heat diffusion, it is equipped with
115 all the necessary elements to be used as a Soil-Vegetation-Atmosphere-Transfer model. This precise
quality made it possible to use summer data like the ones collected at Norunda for a more thourough
validation of the model : indeed, we couldn't find any record of tree temperature measurements
performed in winter environments that would be as long (3 months) and as exhaustive as the
Norunda data. The latter include the monitoring of tree temperature and air temperature at
120 different heights, and a careful calculation of biomass and biomass+air heat fluxes based on
measurements and theoretical considerations. In comparison, the tree temperature and long-wave
irradiance data by Pomeroy et al. (2009) only cover two 3-to-4 days periods.

The suitability of SNOWPACK for use in summer context is now specified in Section 4.2 in the revised
manuscript version.

125 • **Mass balance vs energy balance**

4

As the Reviewer mentions, there has been a lot of modelling effort dedicated to the representation of snow in beneath-canopy environments. Lots of them (like Pomeroy et al., 1998) investigated relevant ways to parameterize the interception of solid precipitation and the sublimation loss of the intercepted snow, because they are first-order matters for the snow mass balance and subsequent hydrological applications.

However, at the time when the present study took place, we didn't dispose of new data that would enable to make an important breakthrough in that delicate matter. We therefore chose to revisit data collected earlier (mostly during the SnowMIP2 campaign), part of which could benefit from dedicated additional analyses.

We agree that the model refinements we performed and the model improvement that we diagnosed, are of second order for the snow mass balance when compared to interception issues. We however think that gradually improving model features will, with time, reduce the number of parameters likely to be flawed during a model experiment, so that more relevant conclusions can be drawn as to other critical model parameters like the ones governing interception. In the end, model accuracy should be increased, too.

We try to make the motivations and the philosophy underlying our study more obvious in the introduction and discussion of the revised manuscript.

Since the beginning of our investigations, work has been carried out at SLF-Davos with respect to the parameterization of interception. The first conclusions have just been published this month by Moeser et al.: they bring up new material that will help modellers better constrain interception issues and hence consolidate the model on aspects complementary to the ones we improved. This is now mentionned in the discussion too.

- **« No explicit simulation of snow melt or snow densification in the canopy is included in the model" (p217, ls18-20): why? At least the former is very important, and literature provides ways to do so. You should clearly figure out the effect of the necessary simplifications in the parameterization of Your model contrasting with its physical orientation, mainly cf and the unloading coefficient. »**
We are sorry for the misleading description that made you so critical about our model and dubious as to its physical consistency. Melt of intercepted snow actually occurs as soon as air temperature reaches the snow/rain threshold: intercepted snow then unloads as liquid water, and part of if remains on the leaves as « intercepted liquid water ». The density of intercepted snow also evolves following the conditions of the air surrounding, as described in Lehning et al., 2002a. We reckon that this is not a proper densification process. But because unloading occurs as an excess of the interception capacity (which decreases when the density of intercepted snow increases), warm and humid conditions can naturally trigger snow unloading before the snow-rain threshold in temperature is reached. These processes circumvent some of the limitations that you mentioned.
We modified the manuscript to clarify these processes, as a feedback on your remark.

- **About efficiency criteria:** we thank the reviewer for the enlightening paper by Krause et al. It underlines pretty well the diversity of criterion among which hydrologists can choose or be lost, and their respective strength and weaknesses. Our position in the current paper was to keep things as

5

simple as possible while enabling the reader to build his judgment on the basis of <u>fair and rigorous</u> information.

170 • For the model calibration and evaluation at Alptal we chose a combined criterion based on mean bias MB and root mean square error RMSE :

- MB is crucial to modellers because it can help detect flawed energy or mass-balances, and most more sophisticated efficiency metrics (like Nash Sutcliff Efficiency NSE) are poorly sensitive to such flaws (as underlined among others by Krause et al. 2005).

175 - We insist that although RMSE does not specifically pinpoint errors in synchronicity between signals, it is still sensitive to them, while accounting in a great way for errors in magnitude.

- Additionally, we confess that we also performed our calibration/validation experiments at Alptal using NSE criteria for $LW\downarrow_{BC}$ and $SW\downarrow_{BC}$: this resulted in the selection of the same model parameters than the calibration based on our combined criteria, while the difference in

180 numerical values between the different model versions was less striking and the main effects brought by the new model versions (reduction in LW bias) was harder to identify.

- Absolute errors (in radiation budgets for our case) matter more to us than relative ones du to their impact on the energy balance, hence no use of relative efficiency index in our study.

• For the model evaluation against biomass heat fluxes at Norunda, we kept the same line of

185 simplicity and fairness in the evaluation metrics provided to the reader. With respect to the metrics provided at Alptal, we provided the correlation coefficient (corr) because the RMSE errors were on the order of magnitude of the model standard deviation, questioning more directly the appropriate periodicity of the signal. The use of « corr » provided insight into that. Furthermore, model evaluation against the combined biomass+air heat flux lead to a desirable improvement in the

190 model-to-data synchronicity, which « corr » also illustrates.

We consider that the mention of the MB, RMSE and corr provides the reader with quite complete and complementary information as to the model quality, equivalent to intercept (linked to MB), slope (indicating goodness in magnitude like RMSE) and R2 (linked to corr) in a model-vs-data scatterplot illustration.

195 For more clarity we also specified in Table 5 that the mean modelled and observed biomass fluxes are null over a period between two equal thermal states.

(ii) Thank you for your detailed advice for the improvement of the English of the manuscript. We considered most of them, with the few following exceptions :

200 - « Physics-based » and « physically based » seem equivalent to us, and « physics-based » is currently in use in diverse papers even in high-rank journals (for instance : http://www.nature.com/nature/journal/v431/n7012/abs/nature02995.html)

- The use of Figure and Fig. within a GMDD manuscript is part of the editing rules.

205 Some questions were also raised in these « Remarks in Details », to which we provide the following answers:

1 .« P222 ls12-22: a bit unclear: do You mean the shadow of the trees at the edge of the forest? »
No. We reformulated our sentence as follows in the manuscript and hope that this is clearer now.

"An exception to that occurs for direct shortwave radiation which is collimated in the solar direction: when sun is not at the zenith, the sun beams are not parallel to the tree trunks and the projected surface occupied by the canopy along their trajectory is higher than (1-c_f)."

2. Ps223 onwards (mainly 2.4.2 and 2.4.3): You should point out clearer what is computed in summer for the atmosphere-canopy-soil continuum, and what in winter when snow is intercepted and/or on the ground. Does the model run continuously all through the seasons and close the water balance? Yes and yes; see answer to (ii) and related modifications in the manuscript.

3. **P241 ls12-19: does this explain why the model reacts faster? According to Your explanation it could be expected that the model peaks later but higher? Please reconsider.**

In our interpretation, it explains why the model reacts faster (i.e. earlier) and also higher. We now detail both mechanism in the manuscript (also copied hereafter), and we were careful to rephrase our original explanation for the sake of clarity. We hope that you understand our interpretation, and welcome any other interpretation that you could suggest or reason why you would disagree.

"We interpret this as an artefact of modelling the canopy with only one or two thermally homogeneous layers, whereas it is in reality a continuous medium experiencing thermal diffusion at scales smaller than our layers. In reality, the low thermal inertia of a bark surface layer provokes quick surface heating as a result of solar energy input (e.g. in the morning). This temporarily limits further heating from turbulent and radiative fluxes, until the surface heat has diffused into the trunk. Contrarily, the bulk, thermally inert trunk layer of our model heats up to a smaller temperature because the heat flux is accommodated by the whole layer and not only by its uppermost surface: further heating by turbulent and radiative fluxes is then still possible and the heat flux towards the biomass keeps being sustained and homogeneously distributed in the layer. As a result, our modelled canopy accommodates incoming energy more rapidly than a real one during the first part of the diurnal cycle. The aforementioned mechanism can also cause the accommodation of more heat energy by the modeled trunk layer than in reality: in reality, the capacity of the canopy to accommodate heat is somewhat limited by thermal diffusion, and heat uptake stops when available solar energy starts going down. At that time, the wooden medium has usually not reached an homogeneous (high) temperature yet (e.g. Fig 1 from Lindroth et al., 2010)."

Point-by-point response to comments by Referee # 2:

240   Thank you for your kind encouragements and enthusiastic welcome of our work!

1. As a response to your Point 1, please consider Fig 3 and 4 of this response, displaying the model-to-data RMSE (Root Mean Square Error) in SWE (Snow Water Equivalent) as a function of *laifrac* (fraction of LAI attributed to the leafy layer, f_{LAI} in the manuscript model description) and *krnt* (short-waves extinction coefficient of the whole canopy, k_{LAI} in the
245   manuscript model description). These results are obtained using the 2-layer canopy model. We focused on snow-years 2004-2005 and snow-years 2006-2007, because there is high suspicion of flawed precipitation data in the other years with available data at Alptal, as stated in the manuscript. For comparison, the model-to-data RMSE obtained with the other one-layered model versions are given in the caption.
250

These figures illustrate that there is quite a wide domain where parameters *laifrac* and *krnt* lead to a RMSE with respect to snow observations as low as possible, and that the chosen *laifrac* and *krnt* values (as a result of calibration against radiation data) are within this domain (for 2006-2007) or very close to it (for 2004-2005), where variability remains quite
255   low. With these values, the model-to-data RMSE in SWE is definetly lower in the 2-layer canopy model than with the 1-layered versions.
We insist here that calibration against radiation data enabled the use of more years due to higher reliability of the data (cf. the suspicion of flaws in precipitation data); it also enabled the calibration of parameters directly linked to the radiation transmission/absorption
260   scheme of the model, whereas calibration against SWE data would have relied on additional hypotheses regarding snow interception and rain-snow partitioning.
However, highlighting the relatively low sensitivity of the modelled SWE to variations of *krnt* and *laifrac* around their optimum values strengthens our confidence in the model robustness. We thank the reviewer for this helpful comment and mentioned this additional
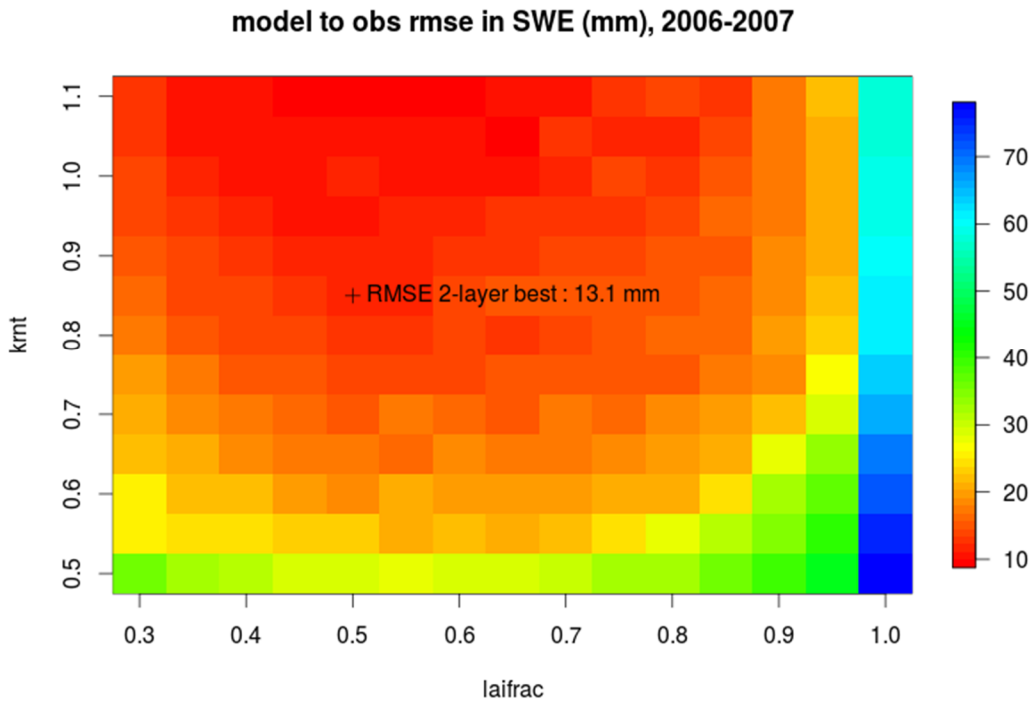265   result in the revised manuscript.

2. We took your helpful comment into account and modified Fig.3 of the manuscript accordingly.

270   3. The expression has been changed.

4 and 5: the grammatical mistake has been corrected and the ambiguous sentences have been changed with a view of enhanced clarity.

8

model to obs rmse in SWE (mm), 2006-2007

+ RMSE 2-layer best : 13.1 mm

Fig 3. RMSE between modelled SWE and observed SWE at Alptal (2006-2007) as a function of 2 model parameters: *krnt* and *laifrac*. The cross over the plot indicates the result of the calibration of the 2-layer model for these parameters for the long 2003-2007 period (Table 4 of the manuscript). As an indication, the calibrated one-layer model versions (1LnoHM and 1LHM) yield RMSE to observations of 34.9 mm and 64.5 mm, respectively.
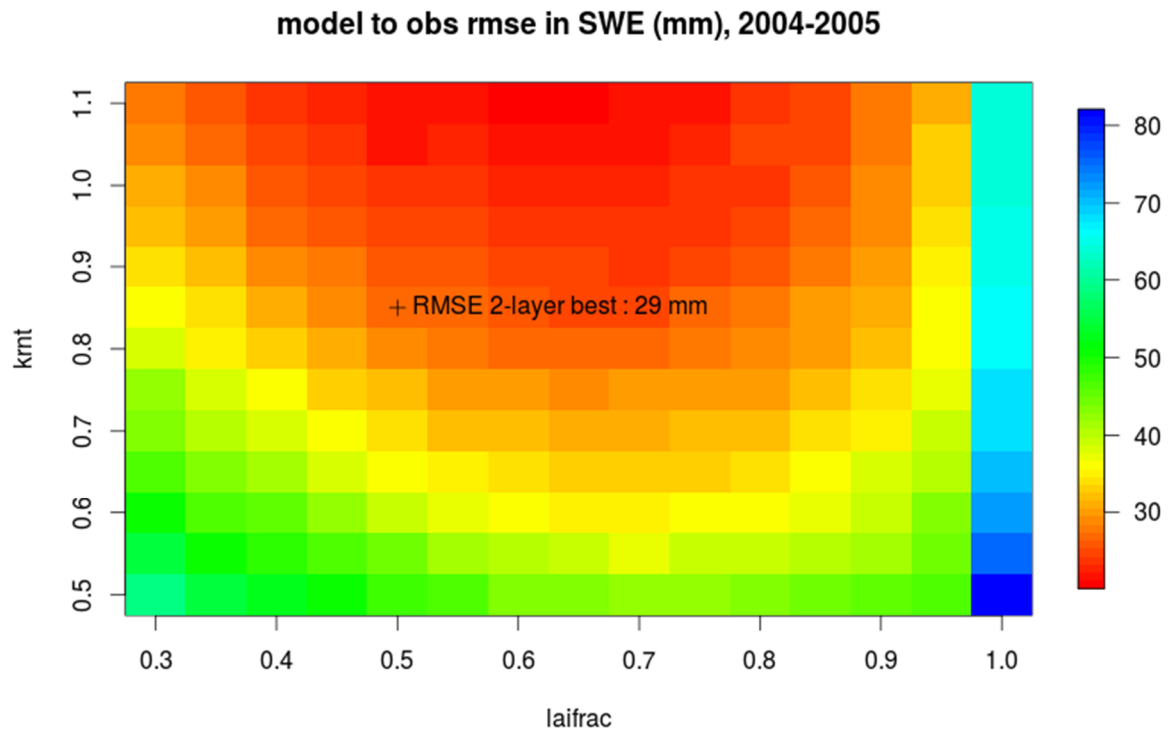
model to obs rmse in SWE (mm), 2004-2005

Fig 4. Same as Fig. 3 but for snow year (2004-2005). The calibrated one-layer model versions (1LnoHM and 1LHM) yield RMSE to observations of 39 mm and 77 mm, respectively.

References

Durot, K. Modélisation hydrologique distribuée du bassin versant pluvio-nival de Sarennes. Validation des données d'entrée et développement d'un module de fonte nivale sous foret (in French). PhD thesis, Institut National Polytechnique de Grenoble, Grenoble, 1999.

Lehning, M., Bartelt, P., Brown, B., and Fierz, C.: A physical SNOWPACK model for the Swiss avalanche warning: Part III: Meteorological forcing, thin layer formation and evaluation, Cold Reg. Sci. Technol., 35, 169–184, 2002a.

Moeser, D., Staeli, M. and Jonas, T. : Improved snow interception modeling using canopy parameters derived from airborne LIDAR data. Wat. Resour. Res., Accepted Article, doi: 10.1002/2014WR016724, 2015.

Pomeroy, J. W., Marks, D., Link, T., Ellis, C., Hardy, J., Rowlands, A., and Granger, R.: The impact of coniferous forest temperature on incoming longwave radiation to melting snow, Hydrol. Process., 23, 2513–2525, 2009.

Pomeroy, J. W., Parviainen, J., Hedstrom, N., and Gray, D.: Coupled modelling of forest snow interception and sublimation, Hydrol. Process., 12, 2317–2337, 1998.

A two-layer canopy model with thermal inertia for an improved snowpack energy-balance below needleleaf forest (model SNOWPACK, version 3.2.1, revision 741)

305   I. Gouttevin[1,2], M. Lehning[2,3], T. Jonas[3], D. Gustafsson[4], M. Mölder[5]

[1] IRSTEA, Unité de Recherche Hydrologie-Hydraulique, 5 rue de la Doua, CS 70077, 69626 Villeurbanne Cedex, France

[2] CRYOS, School of Architecture, Civil and Environmental Engineering, EPFL, Lausanne, Switzerland

310   [3] WSL Institute for Snow and Avalanche Research SLF, Flüelastrasse 11, 7260 Davos Dorf, Switzerland

[4] KTH, Department of Land and Water Resources engineering, Stockholm, Sweden

[5] Lund University, Department of Physical geography and Ecosystem science, Sölvegatan 12, 223 62 Lund, Sweden

315   Correspondence: isabelle.gouttevin@irstea.fr

Model: SNOWPACK version 3.2.1, revision 741.

Abstract

320   A new, two-layer canopy module with thermal inertia as part of the detailed snow model SNOWPACK (version 3.2.1) is presented and evaluated. As a by-product of these new developments, an exhaustive description of the canopy module of the SNOWPACK model is provided, thereby filling a gap in the existing literature.

In its current form, the two-layer canopy module is suited for evergreen needleleaf forest, with or
325   without snow-cover. It is designed to reproduce the difference in thermal response between leafy and woody canopy elements, and their impact on the underlying snowpack or ground surface energy balance. Given the number of processes resolved, the SNOWPACK model with its enhanced canopy module constitutes a very advanced, physics-based modelling chain of the continuum going from atmosphere to soil through the canopy and snow.

330   Comparisons of modelled sub-canopy thermal radiation to stand-scale observations at an Alpine site (Alptal, Switzerland) demonstrate improvements imputable to the new canopy module. Both thermal heat mass and the two-layer canopy formulation contribute to reduce the daily amplitude of the modelled canopy temperature signal, in agreement with observations. Particularly striking is the attenuation of the night-time drop in canopy temperature, which was a key model bias. We
335   specifically show that a single-layered canopy model is unable to produce this limited temperature drop correctly.

The impact of the new parameterizations on the modelled dynamics of the sub-canopy snowpack is analysed. The new canopy module yields consistent results but the frequent occurrence of mixed-precipitation events at Alptal prevents a conclusive assessment of model performance against snow
340   data.

The new model is also successfully tested without specific tuning against measured tree temperature and biomass heat storage fluxes at the boreal site of Norunda (Sweden). This provides an independent assessment of its physical consistency and stresses the robustness and transferability of the chosen parameterizations.

345   The SNOWPACK code including the new canopy module is available under GPL license and upon creation of an account at https://models.slf.ch/.

1   Introduction

350   In the Northern Hemisphere, around 19 % of the annually snow-covered areas are forested (Rutter et al., 2009). As this type of ecosystem has considerable implications for the mass and energy balance of the surface snowpack (e.g. Harding and Pomeroy, 1996; Otterman et al., 1988), the proper understanding and representation of the snow-canopy interactions is crucial whenever realistic estimates of snow cover and melt dynamics in forested environments are needed. This is specifically
355   of concern for hydrological modelling at all scales, runoff estimates from poorly gauged catchments, flood and drought forecasting, global water budget assessment, and in support of local water resources management including irrigation, provision of drinking water, industrial, touristic or hydropower applications.

Also, the snowpack insulates the underlying soil from winter cold air temperature, with implications
360   for the ecosystem in terms of vegetation cover and dynamics (Rasmus et al., 2011; Grippa et al., 2005), litter decomposition (e.g. Saccone et al., 2013) or carbon cycling (e.g. Kelley et al., 1968). The representation of this insulation is one of the critical uncertainties of the modelling of the global soil carbon cycle and its evolution in permafrost environments (Lawrence and Slater, 2010; Gouttevin et al., 2012). The northwards migration of shrubs observed in the last decades at high latitudes (e.g.
365   ACIA 2005) also indicates that snow-forest interactions are to become more and more a concern for climate modelling in the context of global warming.

The insulation properties of snow depend on snow depth and snow thermal conductivity, which in the end relates to the type, characteristics and spatial arrangement of snow crystals within the snowpack. The realistic description of these parameters can hence be a prerequisite for a reliable
370   representation of soil thermal regime and microbiological processes. Snow stratigraphy is also of concern for specific local activities like reindeer grazing in northern countries (Tyler et al., 2010; Vikhamar-Schuler et al., 2013). At present, to the authors' knowledge, such a description is rarely provided by modelling tools for sub-canopy snowpacks (Rasmus et al., 2007; Tribbeck et al. 2006).

Several processes affect the snow cover in sub-canopy environments when compared to open sites.
375   Snow interception by dense canopies and subsequent sublimation or melt of intercepted snow can reduce sub-canopy snow accumulation by up to 60 % (Hardy et al., 1997). Conversely, canopy shading from solar shortwave radiation (SW) can lead to longer-lasting snow cover in forested environments, while enhanced long-wave emission (LW) from sunlit trees with low albedo can have the reverse effect (Sicart et al., 2004; Strasser et al., 2011; Lundquist et al., 2013). In such an
380   environment, effects by topographical shading, solar angle, canopy structure, and understory further complicate the matters. Sub-canopy snow is additionally sheltered from wind, thereby experiencing reduced turbulent fluxes. Finally, canopy debris tend to accumulate over the snow and modify its optic properties on the course of the season.

This complexity makes the understanding and prediction of the sub-canopy snow cover evolution a
385   challenging task. As a result, generations of modellers have worked to capture how canopies affect the micro-meteorological conditions above snow, and predict the resulting evolution of sub-canopy snow (e.g. Essery, 1998; Pomeroy et al., 1998; Durot 1999; Liston and Elder, 2006; Rutter et al., 2009; Strasser et al., 2011). The first focus of this modelling was usually on snow interception, interception evaporation and (lack of) snow redistribution, as major features shaping the amount of snow
390   beneath canopies (Essery, 1998; Pomeroy et al., 1998). Later, the sub-canopy or within-canopy

micro-meteorology was increasingly refined to include a representation of temperature, radiation and turbulent fluxes: Durot (1999) initiated a treatment of the meteorological fields provided by the French analysis SAFRAN to translate them into sub-canopy fields. This involved an homothetic transformation of the air temperature, an increase in air humidity, a formulation for turbulent fluxes in canopy-dampened wind conditions, and the shading from solar radiation through a Beer-Lambert or a linear law. Later, Jansson and Karlberg (2001), Yamazaki (2001), Tribbeck et al. (2004, 2006), Liston and Elder (2006) and Strasser et al. (2011) set up dedicated snow models designed for forest environments, featuring different strengths and weaknesses. For instance, the COUP model (Jansson and Karlberg, 2001) features an advanced representation of snow-canopy processes but lacks a detailed, layered snowpack and the associated physical processes. Oppositely, the SNOWCAN model (Tribbeck et al., 2004, 2006) couples a robust radiative transfer model for canopies to the detailed snowpack model SNTHERM, but their treatment of interception is coarse and experimental.

In 2004 and 2009, two significant international intercomparison exercises were compiled to compare the skills of a broad scope of snow models, ranging from land-surface models snow schemes, to very sophisticated models designed for local catchments or point-scale applications (SnowMIP: Etchevers et al. 2004; SnowMIP2: Essery et al. 2008; Rutter et al 2009). They demonstrated the increasing skill of the snow models to capture the dynamics of the sub-canopy snow cover, but highlighted some remaining challenges: misrepresentation of mid-winter melt-events, lack of time-transferability of calibration at forested sites, difficulty to capture the maximum snow accumulation in warm environments, sometimes imputable to unreliable precipitation data. According to Rutter et al. (2009), the former and the latter could be in part due to a coarse representation of mixed precipitation events and rain-on-snow, but also to the misrepresentation of ablation events driven by air temperature rising above 0°C, when models diverge from observations due to their treatment of sub-canopy longwave radiation. In a recent publication, Lundquist et al. (2013) pointed the longwave canopy emissions as the main cause of an early sub-canopy snow melt in snow regions where mean winter temperature exceeds -1°C and mid-winter melt events are frequent. This effect, and the importance of accounting for the thermal structure of different canopy elements, has been pinpointed before by other observation-based studies (Ellis et al. 2013, Pomeroy et al., 2009; Sicart et al., 2004). However, most snow models of the current generation fail to capture it due to an inappropriate treatment of the canopy thermal regime : most of them, like the COUP model or the SNOWPACK model before our work (Bartelt and Lehning 2002, Lehning et al. 2002a, Lehning et al. 2002b, Lehning et al., 2006), use the above-canopy air temperature as a substitute for canopy temperature. There are few exceptions, though: In their design of a land surface model dedicated to intensively cold regions, Yamazaki et al. (1992, Yamazaki, 2001) resolve a separate energy balance for two canopy layers (crown and trunks). However, they do not compare their results to canopy temperature or radiation data, nor do they assess the added value of this specific model design for the sub-canopy snow surface energy balance. In the afore-mentioned SNOWCAN and in SnowModel (Liston and Elder, 2006), an observed or hypothesized canopy temperature can be used as a model input to compute the thermal emission of the canopy and its impact on sub-canopy snowmelt. However, this is not a comprehensive modelling approach, that would suppose to compute the canopy temperature by itself. In ADMUNSEN, Strasser et al. (2011) uses the heuristic formulation by Durot (1999) which accounts for thermal dampening by the canopy, but do not propose a physical formulation of the canopy temperature. This approach may show some limitations in specific meteorological conditions or in discontinuous forest where trunks are exposed to direct solar radiation.

Our work here builds on the hypothesis by Rutter et al. (2009). We aim at testing the improvements induced to the sub-canopy energy balance by a physically-consistent formulation of the canopy thermal structure and the distinction between woody and leafy elements. Focus is mostly on snow-covered environments, but not exclusively. For our purpose, we develop a 2-layer canopy representation (leaves and wood) in the aforementioned SNOWPACK model. SNOWPACK proposes a very detailed, physical and microphysical representation of the snowpack. Before our work, it included a simple, one-layer canopy module where radiation and precipitation interception by forest elements were represented (e.g. Musselmann et al., 2012), but the equivalence between air and canopy temperature was assumed. Because SNOWPACK was initially developed for alpine environment and is still mostly used in alpine or boreal context where conifers are dominants, our new canopy module is for now only suited for needleleaf, evergreen forest.

Micro-meteorological and sub-canopy, stand-scale radiation data collected during the SnowMIP2 experiment build a proper dataset for the evaluation of our developments. We complement them with tree trunk temperature and biomass flux measurements collected in a summer boreal environment, which is an interesting test-case for model transferability and robustness.

Our contribution is hence structured in the following way:

4. an exhaustive documentation of the new model and the canopy module it is embedded in, is proposed, for the sake of clarity and knowledge dissemination. Earlier versions of the canopy module had been only partially described in Stähli et al. (2006) and in appendix A of Musselmann et al. (2012).

5. existing simultaneous observations of sub-canopy radiation, snow evolution and meteorological conditions from Alptal (Switzerland) are used to validate the new model and demonstrate its robustness and improvement over simpler canopy formulations and with respect to observations.

6. model validity and transferability is finally tested against observations of components of the canopy energy balance taken from a different coniferous environment (Norunda, Sweden).

2 Model description

2.1 The SNOWPACK / Alpine3D snow model

SNOWPACK is a one-dimensional, physics-based snow-cover model originally dedicated to avalanche risk assessment. Driven by standard meteorological observations, the model describes the stratigraphy, snow microstructure, snow metamorphism, temperature distribution, and settlement as well as surface energy exchange and mass balance of a seasonal snow cover. It has been extensively described in Bartelt and Lehning (2002) and Lehning et al. (2002a, b). Since 2005, it also includes the effect of vegetation above and within or below the snowpack.

Snowpack can be wrapped into an open-source, spatially distributed, 3-dimensional model for analyzing and predicting the dynamics of snow-dominated surface processes in complex alpine topographies: Alpine3D (Lehning et al., 2006). In addition to SNOWPACK, Alpine3D includes a preprocessing and interpolation module for meteorological fields (Bavay & Egger, 2014), a module computing the spatially distributed radiations as affected by topography (Helbig et al., 2009), an optional snow transport model (Groot et al., 2011) and an optional runoff model (Zappa et al., 2003;

Comola et al., 2015). The interpolated or provided spatial meteorological fields drive the energy and mass balance of the surface snowpack, computed by SNOWPACK. The canopy module and its new features described hereafter can run within Alpine3D. They are included in the SNOWPACK model version 3.2.1 (revisions from 741) which is available under GPL license and upon creation of an account at https://models.slf.ch/.

2.2 The canopy model structure

The canopy module of SNOWPACK calculates the upper boundary conditions for the snowpack or bare soil surface below the canopy. It is based on an energy balance approach in order to be consistent with the distributed radiation scheme used in Alpine3D. Interception and throughfall of precipitation, transpiration and evaporation of intercepted snow or rain as well as the influence of the canopy on radiative and turbulent heat fluxes at the snow or soil surface are included in the model.

In its 1-layer version, the model represents vegetation canopy as a single big-leaf with state variables (i) canopy temperature T_{can} (K) and (ii) storage of intercepted water or snow I (mm). All canopy processes are then computed based on three basic input parameters: canopy height z_{can} (m), leaf area index LAI or plant area index PAI (m^2 m^{-2}), and direct throughfall fraction c_f (-). PAI has more of a physical sense as non-leafy canopy elements play a role in radiative extinction and turbulent fluxes, but PAI and LAI can usually be derived from each other via a factor depending on stand characteristics, thus the switch between both just affects parameter values in our formulations. The description here uses LAI; the direct throughfall fraction can be set to zero if LAI is provided as a stand-scale average including canopy gaps of moderate size (up to ~1 m). These 3 model parameters intend to describe differences between forest stands without further tuning.

The consideration of the thermal inertia of the forest stand in the 1-layer version with heat mass (1LHM) and the 2-layer version (2LHM) imposes the use of an additional input parameter, the mean stand basal area B (m^2 m^{-2}). The different parameters used by the SNOWPACK canopy module are listed in Table 1, distinguishing between the ones to be provided by users according to forest-specificities, and the ones internal to the model.

The idea behind the 2-layer version of the canopy module is to capture the thermal contrast between two distinct compartments of the canopy:

- the upper (or outer) canopy compartment (leaves or needles) which is most directly exposed to the atmosphere
- the lower (or inner) canopy compartment (twigs, branches, trunks, some leaves), for which energy and mass fluxes have already been altered by the upper canopy compartment.

This modelling choice relies on observational data highlighting this contrast and its relevance for the sub-canopy energy balance (Pomeroy et al., 2009). With respect to the 1-layer version, one state variable is added, namely the temperature of the trunk or lower canopy compartment T_{trunk} (K). T_{can} is then replaced by T_{leaves}, the temperature of the upper canopy.

The coupled water and heat balances of the canopy layer are calculated in three steps:

(i) First, a preliminary mass balance is calculated including interception and throughfall of precipitation.

520 (ii) Second, the canopy temperature T_{can} is calculated by solving the energy balance of the canopy. For this purpose, all the non-linear energy fluxes to the canopy have been linearized in terms of canopy temperature via Taylor series. The radiation transfer and turbulent exchange of sensible and latent heat are then deduced. For the 2-layer version, the energy balance of the upper canopy also includes thermal emission from the lower canopy which is

525 similarly linearized in terms of T_{can} via the explicit formulation of an energy balance for the lower canopy.

(iii) Third, the mass balance of the canopy is updated by the evaporation (or condensation) calculated in step two.

The 2-layer version affects the canopy energy balance and computation of net radiation in each

530 layer. For the sake of simplicity the 1-layer canopy module is first fully described. The specificities implied by the consideration of two layers are then dealt with in the last part of this section.

2.3 Interception parameterization

The mass balance of the canopy layer includes three fluxes of water: interception of precipitation ΔI

535 (mm day^{-1}), interception evaporation E_{int} (mm d^{-1}) and water unloading from the canopy U (mm d^{-1}):

$$dI/dt = \Delta I - E_{int} - U . \tag{1}$$

where I (mm) is the interception storage.

A fraction $(1-c_f)$ of the precipitation P (mm day^{-1}) is available for interception at each time step. The interception rate is calculated as a function of canopy storage saturation with an equation originally proposed by Merriam (1960), in the form given by Pomeroy et al. (1998):

$$\Delta I = c(I_{max} - I)\left(1 - \exp\left\{-\frac{(1-c_f)P}{I_{max}}\right\}\right) . \tag{2}$$

540 where the parameter c (-) is a model time-step dependent parameter known as the unloading coefficient. Pomeroy et al. (1998) suggested a value of $c = 0.7$ appropriate for hourly time-steps. Canopy interception capacity I_{max} (mm) is assumed to be proportional to leaf area index:

$$I_{max} = i_{LAI} LAI \tag{3}$$

where the parameter i_{LAI} (mm) is either set to a constant corresponding to the interception capacity for liquid precipitation when these occur, or parameterized as a function of snow density during

545 snowfall events, following Pomeroy et al. (1998):

$$i_{LAI} = i_{max}(0.27 + 46/\rho_{s,int}) . \tag{4}$$

Schmidt and Gluns (1991) reported estimates of the parameter i_{max} (mm) for spruce (5.9) and pine (6.6). The density of the intercepted snow $\rho_{s,int}$ (kg m^{-3}) is estimated as a function of air temperature (Lehning et al.,2002b). Different values have been reported for the interception capacity of snow, depending on forest type and climate (e.g. Koivusalo et al., 2002; Essery et al., 2003). Most

550 important is to recognize the large difference between solid and liquid precipitation. The phase of the intercepted water is assumed to be equal to the phase of precipitation at each timestep. A

mixture of liquid water and snow can therefore form the interception storage, and unloading proceeds as the interception capacity of the needles decreases with the enhanced density of the intercepted mixture or with a shift towards positive temperatures.

555 The partition of precipitation into snowfall and rainfall in SNOWPACK depends on available data. Usually precipitation with undistinguished phase is used, and a temperature threshold disentangles the phases with linear or logistic smoothing around the threshold (Kavetski and Kuczera, 2007). When phase information is available and mixed events occur, the interception capacity is calculated according to Eq. (4), but using the weighed sum of liquid water and new snow density instead of the
560 density of snow. For rain-only or snow-only events, Eq. (3) and (4) are respectively used without change.

Different approaches have been proposed for calculations of snow unload from the canopy: Essery et al. (2003) set the unload rate equal to a fraction (40 %) of calculated melt of intercepted snow. Koivusalo and Kokkonen (2002) assumed that all intercepted snow unloads as soon as the air
565 temperature rises above 0°C. We have chosen to calculate snow unload U (mm day^{-1}) only when the interception storage exceeds the actual interception capacity:

$$U = max[0, I - I_{max}] / \Delta t,$$
(5)

which happens when the interception capacity is reduced due to the precipitation of heavy, wet snow or due to an increase in air temperature. Sudden release of large amount of snow is thus avoided since the intercepted snow density is increased gradually towards the threshold air
570 temperature for snowfall. This is favorable for the numerical stability of the snowpack simulation. This simple parameterization also respects the fact that individual branches usually release snow at a time and total unloading of a whole tree is not very frequent.

Throughfall T (mm day^{-1}) to the forest floor is thus equal to:

$$T = P - \Delta I + U$$
(6)

Evaporation of intercepted water is calculated as part of the canopy energy balance (cf. below) and
575 added to the water balance at the end of the model time step.

2.4 Canopy energy balance

The canopy temperature is directly derived from the canopy energy balance.

The 1-layer canopy module with no heat mass (1LnoHM, e.g. the version used in previous modelling
580 studies: Rutter et al. 2009, Musselmann et al., 2012) relies on an assumption of stationarity, whereby net radiation of the canopy $R_{net,can}$ (W m^{-2}) is assumed to equal the sum of sensible H_{can} (W m^{-2}) and latent LE_{can} (W m^{-2}) heat fluxes neglecting any storage or sources/sinks of heat within the canopy:

$$R_{net,can} = H_{can} + LE_{can}$$
(7)

In the new canopy module, 1 layer version with heat mass, (1LHM) the thermal inertia of trees is
585 accounted for via a biomass storage flux BM_{can} (W m^{-1}), modifying the canopy energy balance :

$$R_{net,can} = H_{can} + LE_{can} + BM_{can}$$
(8)

2.4.1 Radiation transfer

A radiation transfer model for a single canopy layer above a snow or bare soil surface has been adopted from Taconet et al. (1986) by Stähli et al (2009). The model assumes a fractional absorption of radiation in the canopy layer given by the absorption factor σ_f (-). A fraction of the absorbed radiation is reflected, as defined by the reflection factors for shortwave (albedo) and longwave radiation, respectively. Radiation transmitted to the surface below is absorbed and reflected according to the corresponding reflection factors for the surface.

Following these basic assumptions, and integrating n multiple reflections between the canopy layer and the underlying surface, the net shortwave radiation absorbed by the canopy layer $SW_{net,can}$ (W m^{-2}) is given by:

$$SW_{net,can} = SW_\downarrow - \sigma_f \alpha_{can} SW_\downarrow - (1-\sigma_f)SW_\downarrow \tag{9}$$

$$+ \sum_{n=1}^{\infty} (\alpha_{surf})^n (\sigma_f \alpha_{can})^{n-1}(1-\sigma_f)SW_\downarrow$$

$$- \sum_{n=1}^{\infty} (\alpha_{surf})^n (\sigma_f \alpha_{can})^{n}(1-\sigma_f)SW_\downarrow$$

$$- \sum_{n=1}^{\infty} (\alpha_{surf})^n (\sigma_f \alpha_{can})^{n-1}(1-\sigma_f)^2 SW_\downarrow$$

where $SW_\downarrow$ (W m^{-2}) is the incoming shortwave radiation above the canopy layer, and α_{can} (-) and α_{surf} (-) are the albedo of the canopy and the snow/soil surface below, respectively. The first three terms on the right hand side are the incident, reflected, and transmitted downward radiation with regard to the canopy layer. The remaining three terms are the sums of incident, reflected and transmitted upward radiation, as a result of multiple reflections between the canopy and the surface below. Equation (9) can be simplified to:

$$SW_{net,can} = SW_\downarrow (1-\alpha_{can})\sigma_f \left(1 + \frac{\alpha_{surf}(1-\sigma_f)}{1-\sigma_f \alpha_{surf}\alpha_{can}}\right) \tag{10}$$

by mathematical relationships for geometric series. The same procedure can be applied for net shortwave radiation absorbed by the ground surface $SW_{net,surf}$ (W m^{-2}) which thus can be written as:

$$SW_{net,surf} = \frac{SW_\downarrow (1-\alpha_{surf})(1-\sigma_f)}{1-\sigma_f \alpha_{surf}\alpha_{can}} \tag{11}$$

The calculation of the longwave radiation is further simplified by assuming an emissivity equal to 1, giving the following equations for net longwave radiation absorbed by the canopy $LW_{net,can}$ (W m^{-2}), and the ground surface $LW_{net,surf}$ (W m^{-2}),:

$$LW_{net,can} = \sigma_f (LW_\downarrow + \sigma T_{surf}^4 - 2\sigma T_{can}^4) \tag{12}$$

$$LW_{net,surf} = (1-\sigma_f)LW_\downarrow + \sigma_f \sigma T_{can}^4 - \sigma T_{surf}^4 \tag{13}$$

where σ is the Stefan-Boltzmann constant $5.67 \cdot 10^{-8}$ W m^{-2} K^{-4} and $LW_\downarrow$ is the thermal radiation from the sky. Neglecting the emissivity might overestimate the loss and gain of thermal radiation from the canopy. On the other hand, the absorption factor σ_f (-) has a similar effect on the net adsorption/emittance, and it may be difficult to separate these two properties.

The net radiation to the canopy is then the sum of the LW and SW net contributions:

$$R_{net,can} = SW_{net,can} + LW_{net,can} \tag{14}$$

The albedo of the canopy α_{can} (-) is equal to:

$$\alpha_{can} = f_{wet}\alpha_{wet} + (1 - f_{wet})\alpha_{dry} \tag{15}$$

where f_{wet} (-) is the fraction of the canopy covered by intercepted water calculated as:

$$f_{wet} = (I / I_{max})^{2/3}, \tag{16}$$

and α_{wet} (-) and α_{dry} (-) are the albedo of wet and dry canopy, respectively. The albedo for the wet part of the canopy can be set differently for liquid and solid interception (Table 1).

The canopy absorption factor σ_f (-) is assumed to be equal for longwave and diffuse shortwave radiation, independent of interception storage and phase, and is calculated as a function of LAI:

$$\sigma_f = 1 - \exp\{-k_{LAI}LAI\} \tag{17}$$

where k_{LAI} (-) is an extinction parameter with values normally between 0.4-0.8.

For direct shortwave radiation, it can optionally be a function of solar elevation angle ϑ_{elev}, following Chen et al. (1997):

$$\sigma_{f,dir} = 1 - \exp\left\{-\frac{k_{LAI}LAI}{\sin(\theta_{elev})}\right\} \tag{18}$$

where ϑ_{elev} is limited to the range [0.001-π/2] to ensure a positive value of $\sigma_{f,dir}$.

Direct and diffuse SW radiations are in this case disentangled by the model after Erbs et al. (1982).

For the sake of completeness, the effective surface albedo, α_{total} (-), and radiative surface temperature, T_{eff} (K) above the canopy layer are given as:

$$\alpha_{total} = \alpha_{can}\sigma_f + \alpha_{surf}\frac{(1 - \sigma_f)^2}{1 - \alpha_{can}\alpha_{surf}\sigma_f} \tag{19}$$

and

$$T_{eff} = \left(\frac{LW_\downarrow - LW_{net,can} - LW_{net,surf}}{\sigma}\right)^{0.25} \tag{20}$$

respectively. These variables have no influence on the 1D-simulations presented here, but are used to estimate the contribution of longwave and shortwave radiation from surrounding terrain when the SNOWPACK model is used within the distributed Alpine3D model.

Finally, the radiation fluxes calculated by the canopy module are only applied to the fraction of the surface covered by the canopy, assumed to be the complement of the direct throughfall parameter:

This higher fraction of canopy shading ($1-c_{f,dir}$) is derived following Gryning et al. (2001) from the mean canopy height z_{can} (m) and an average canopy diameter D_{can} (1 m by default):

$$1 - c_{f,dir} = Min\left[1, (1 - c_f) \cdot \left(1 + \frac{4 \times z_{can}}{\pi . D_{can} . \tan(\theta_{elev})}\right)\right] \tag{21}$$

In the remaining fraction of the surface, the exchange of longwave and shortwave radiation between the atmosphere and the ground surface is calculated without influence of the canopy.

2.4.2 Turbulent fluxes

The turbulent fluxes of sensible and latent heat from the canopy to the reference level of the meteorological input (above the canopy) are calculated using the bulk formulation:

$$H_{can} = \frac{\rho c_p}{r_H}(T_{can} - T_{air}) \tag{22}$$

$$LE_{can} = \frac{0.622 L}{R_a T_{air}} \frac{1}{r_E}(e_{sat}[T_{can}] - e_{air}) \tag{23}$$

where ρ (kg m^{-3}) and c_p (J kg^{-1} K^{-1}) are the density and heat capacity of air, T_{can} (K) is the canopy layer temperature, T_{air} (K) and e_{air} (Pa) are the air temperature and the actual vapour pressure in the air at a reference level z_{ref} (m) above the ground surface, L (J kg^{-1}) is the latent heat of vaporization of water (or sublimation when T_{air} < 273.15 K), R_a is the specific gas constant for air (J kg^{-1} K^{-1}), and $e_{sat}[T_{can}]$ (P$_a$) is the saturated vapour pressure corresponding to the canopy temperature. Furthermore, the turbulent transfer coefficients for heat and vapour are expressed in terms of the aerodynamic resistances r_H (s m^{-1}) and r_E (s m^{-1}) (further described below). Latent heat flux is the sum of transpiration E_{tr} (mm s^{-1}) and evaporation of intercepted water E_{int} (mm s^{-1}). The partitioning of the components from partly wet canopies can be a delicate problem. To simplify the numerical solution of the energy balance, we have chosen to formulate an effective aerodynamic resistance r_E for latent heat calculated as an average of the corresponding values for transpiration r_{Etr} and interception evaporation r_{Eint}, weighted by the fraction of wet canopy f_{wet}:

$$\frac{1}{r_E} = \frac{1}{r_{Eint}}f_{wet} + \frac{1}{r_{Etr}}(1 - f_{wet}) \tag{24}$$

The total evaporation E_{can} (m day^{-1}) is calculated directly (Eq. (23)), and its components are derived as secondary results:

$$E_{int} = E_{can}\frac{r_E}{r_{Eint}}f_{wet} \tag{25}$$

$$E_{tr} = E_{can}\frac{r_E}{r_{Etr}}(1 - f_{wet}) \tag{26}$$

The derivation of the aerodynamic resistances for transpiration and interception evaporation is given in the next section. Transpiration is not allowed if the achieved E_{can} is negative (condensation). In such cases, the solution of the energy balance has to be re-calculated using $f_{wet}=1$.

660 At temperatures below the freezing point the modelled canopies do not transpire anymore. If the canopy energy balance forces, through Eq. (24), an evaporation that cannot be sustained by the interception storage, the latter limits the possible evaporation and the canopy energy balance is recalculated accordingly.

665 2.4.3 Aerodynamic resistances

The aerodynamic resistances for sensible and latent heat fluxes are calculated using a two-layer model adapted from Blyth et al. (1999) which for simplicity assumes logarithmic or log-linear wind profiles both above, within, and below the canopy. More elaborate models have been suggested by for instance Shuttleworth and Wallace (1985), however, the remaining

670 uncertainties in the representation of the within-canopy turbulent exchange call for a simple approach. The aerodynamic resistance for scalars from the canopy level, defined by the displacement height d (m), to the reference level of the wind and temperature measurements z_{ref} above the canopy, is calculated as:

$$1/r_{air} = u_* k / \left(\ln\left(\frac{z_{ref} - d}{z_{0m}}\right) + \psi_h \right) + c_{h0}/(\rho c_p)$$

(27)

where u_* (m s^{-1}) is the friction velocity:

$$u_* = u_{ref} k / \left(\ln\left(\frac{z_{ref} - d}{z_{0m}}\right) + \psi_m \right)$$

(28)

675 k is the Karman constant (0.4), z_{0h} (m) and z_{0m} (m) are the canopy roughness lengths for heat and momentum, ψ_m (-) and ψ_h (-) are functions correcting for atmospheric stability following Högstrom (1996) and Beljaars and Holtslag (1991). In addition to Blyth et al. (1999), and following e.g. Koivusalo and Kokkonen (2002), we introduce an additional parameter c_{h0} (W m^{-2} K^{-1}) representing a minimum heat exchange coefficient for windless conditions. Displacement

680 height, and canopy surface roughness length of momentum and heat are related to the canopy height through the parameters f_d (-), f_{z0m} (-), and $f_{z0h/z0m}$ (-) with values given in Table 1:

$$d = f_d z_{can}$$

(29)

$$z_{0m} = f_{z0m} z_{can}$$

(30)

$$z_{0h} = f_{z0h/z0m} z_{0m}$$

(31)

In addition to the resistance between the canopy air (canopy reference level) and the reference level for meteorological measurements (above the canopy), excess resistances from the canopy surface, and from the soil/snow surface (beneath the canopy), to the canopy level are defined as:

$$r_{can} = \ln\left(\frac{z_{0m}}{z_{0h}}\right)\frac{1}{u_* k} \tag{32}$$

$$r_{surf} = \ln\left(\frac{z_{0m}}{z_{0h,surf}}\right)\frac{1}{u_* k} f_{surf} \tag{33}$$

685   There, a multiplicative increase of the resistance below the canopy f_{surf} (-) is introduced as a function of the leaf area index:

$$f_{surf} = 1 + r_{a,LAI}\left(1 - \exp\{-LAI\}\right) \tag{34}$$

with a maximum value of $1 + r_{a,LAI}$ (-). The excess surface resistance below the canopy, r_{surf}, affects the heat and latent fluxes computed from the ground to the reference level. This resistance is corrected for atmospheric stability by applying the same stability functions as in Eq. (27) and (28), but in this
690   case using the temperature difference between the canopy and the snow or bare soil surface instead of the temperature difference between the canopy and the air. With the current choice of parameter values, the excess resistance for the canopy surface is almost zero, but the theoretical framework for a later use/optimization of this parameter based on observational data is set.

In the end, the total aerodynamic resistances for heat from the reference level to the canopy and the
695   ground surface, respectively, are given by:

$$r_{H,can} = r_{air} + r_{can} \tag{35}$$

$$r_{H,surf} = r_{air} + r_{surf} \tag{36}$$

The aerodynamic resistances for sensible and latent heat from the ground surface are assumed to be equal. For evaporation from intercepted snow, the resistance from the canopy to the canopy layer can be increased with a factor $f_{ra,snow}$ (-) compared to rain following Lundberg et al. (1998) and Koivusalo and Kokkonen (2002):

$$r_{Eint} = r_{air} + r_{can} \times \begin{cases} f_{ra,snow} & , T_{air} < 0°C \\ 1 & , T_{air} \geq 0°C \end{cases} \tag{37}$$

700   The total resistance for transpiration also takes the stomatal control into account:

$$r_{Etr} = r_{air} + r_{can} + r_{stomata} \tag{38}$$

where the stomata resistance $r_{stomata}$ (-) is calculated as a function of a minimum resistance r_{smin} (-), incoming solar shortwave radiation, vapour pressure deficit and soil water content θ_{soil} as suggested by Jarvis (1976), and soil temperature T_{soil} following Mellander et al. (2006) and Axelsson and Ågren (1976):

$$r_{stomata} = r_{smin}\frac{f_1[SW_{\downarrow}]f_2[e_{sat} - e_{air}]f_3[\theta_{soil}]f_4[T_{soil}]}{LAI} \tag{39}$$

705   The functions f_1-f_4 in Eq. (39) all take values between 0 and 1, specifying optimal conditions for root water uptake corresponding to the response of the leaf stomata to conditions in the atmosphere and the root zone.

2.4.4 Biomass heat flux

Due to their thermal inertia, trees can store energy over periods of high exposure to solar radiation, and release it at night. This biomass heat flux is accounted for in the 1LHM version of the canopy module via the areal heat mass of trees HM_{can} (J K^{-1} m^{-2}):

$$BM_{can} = HM_{can} \cdot \frac{T^t_{can} - T^{t-1}_{can}}{\Delta t} \tag{40}$$

where T^t_{can} (K) and T^{t-1}_{can} are the canopy temperature at the model t and $t-1$ timesteps, and Δt (s) is the model timestep. HM_{can} is here derived from parameters commonly observed by foresters: LAI, mean stand basal area B (m^2 m^{-2}) and mean canopy height (z_{can}).

$$HM_{can} = HM_{leaves} + HM_{trunk} \tag{41}$$

$$HM_{leaves} = LAI \; e_{leaf} \; \rho_{biomass} \; C_{p\,biomass} \tag{42}$$

$$HM_{trunk} = 0.5 \; B \; z_{can} \; \rho_{biomass} \; C_{p\,biomass} \tag{43}$$

The leaf thickness e_{leaf} (m), biomass density $\rho_{biomass}$ (kg m^{-3}) and biomass specific heat mass $C_{p\,biomass}$ (J kg^{-1} K^{-1}) are fixed parameters with values 10^{-3}, 900 and 2800 respectively (Lindroth et al., 2010). In Eq. (43), the volume of woody biomass (referred to as "*trunk*" but comprising trunks and branches assimilated to the lower canopy layer) is calculated from mean tree basal area and height assuming a conical profile for trunks. In this study, areal heat masses will be expressed as "water equivalent areal heat masses" HM_{eq} (kg m^{-2}), e.g. as the areal mass of water yielding the same heat mass than HM (J K^{-1} m^{-2}):

$$HM_{eq} = \frac{HM}{C_{p\,water}} \tag{44}$$

where $C_{p\,water}$ = 4181 J kg^{-1} K^{-1} is the liquid water specific heat mass.

2.5 Two-layer canopy version

With respect to the 1-layer canopy module, the 2-layer formulation induces changes in the formulation of radiative transfer, turbulent and biomass fluxes, and in the end the energy balance of the canopy. These differences are the focus of the present paragraph, whereby the upper canopy layer is equivalently referred to as *"leaves"* while the lower canopy layer is labelled *"trunk"*. The formulation of the radiative and turbulent components of the 2-layer module is illustrated in Fig. 1.

2.5.1 Radiative transfer

In a real forest the trunk layer intercepts parts of the shortwave and longwave radiation transmitted, reflected and emitted by the uppermost canopy layer and upwelling from the soil surface.

Our model features a simplified representation of this:

• For SW radiation, only the transmitted radiation from the upper canopy (with absorption factor $\sigma_{fleaves}$ and albedo α_{leaves}) are intercepted or reflected by the trunk layer (with the respective factors σ_{ftrunk} and α_{trunk}). Radiation undergoing multiple reflections between ground surface and upper

canopy are unaffected by the trunk layer (Fig. 1). The SW flux reaching the ground and both canopy layers are expressed accordingly :

$$SW_{net,trunk} = SW_{\downarrow}(1 - \sigma_{f1eaves})(1 - \alpha_{trunk})\sigma_{ftrunk} \tag{45}$$

$$SW_{net,leaves} = SW_{\downarrow}(1 - \alpha_{leaves})\sigma_{fleaves}\left(1 + \frac{\alpha_{surf}(1 - \sigma_{f1eaves})(1 - \sigma_{ftrunk})}{1 - \sigma_{fleaves}\alpha_{surf}\alpha_{trunk}}\right) \tag{46}$$

$$SW_{net,surf,2L} = SW_{\downarrow}\frac{(1 - \sigma_{fleaves})(1 - \sigma_{ftrunk})(1 - \alpha_{surf})}{1 - \sigma_{fleaves}\alpha_{surf}\alpha_{leaves}} \tag{47}$$

740   Obviously, the biomass responsible for SW and LW extinction has now to be split into the two canopy layers so that the total extinction for SW is similar in both versions. Equating the first order radiation from Eq. (11) and (47) yields:

$$(1 - \sigma_f) = (1 - \sigma_{fleaves}).(1 - \sigma_{ftrunk}) \tag{48}$$

Or equivalently, based on (17):

$$LAI = LAI_{leaves} + LAI_{trunk} \tag{49}$$

where LAI_{leaves} and LAI_{trunk} are the respective portions of the total LAI attributable to the upper and
745   lower canopies. We denote hereafter

$$f_{LAI} = \frac{LAI_{leaves}}{LAI} \tag{50}$$

and express the leaves-layer and trunk-layer absorption factors as functions of LAI and f_{LAI}:

$$\sigma_{fleaves} = 1 - \exp\{-k_{LAI} f_{LAI}.LAI\} \tag{51}$$

$$\sigma_{ftrunk} = 1 - \exp\{-k_{LAI}(1 - f_{LAI}).LAI\} \tag{52}$$

Similarly to the 1-layer version (Eq. (18)), these factors can be adapted to enhance absorption of direct SW radiation based on solar elevation angle.

f_{LAI} is an a priori undetermined parameter of our model due to the difficulty of deriving it from of
750   existing datasets for different forest types and structures. In Sect. 4, we show that the calibration of the model at Alptal against this parameter yields $f_{LAI} = 0.5$, which means equal contribution from the woody and leafy parts of the forest to shortwave extinctions. This value is adopted as default value in the model (see Sect. 5 for discussion).

• For LW radiation, the choice of an emissivity of 1.0 for ground and canopy suppresses multiple
755   reflections. Thermal emission from the upper canopy layer and from the ground is attenuated by the trunk layer with the same absorption factor as for SW radiation σ_{ftrunk}. The trunk layer then radiates thermally towards the ground and the upper canopy layer and sky.

$$LW_{net,trunk} = \sigma_{ftrunk}\left(LW_{\downarrow}(1 - \sigma_{fleaves}) + \sigma T_{surf}^4 + \sigma_{fleaves}\sigma T_{leaves}^4 - 2\sigma T_{trunk}^4\right) \tag{53}$$

$$LW_{net,leaves} = \sigma_{fleaves}\left(LW_{\downarrow} + \sigma T_{surf}^4(1 - \sigma_{ftrunk}) + \sigma_{ftrunk}\sigma T_{trunk}^4 - 2\sigma T_{leaves}^4\right) \tag{54}$$

$$LW_{net,surf,2L} = (1 - \sigma_{fleaves})(1 - \sigma_{ftrunk})LW_{\downarrow} + \sigma_{fleaves}(1 - \sigma_{ftrunk})\sigma T_{leaves}^4 + \sigma_{ftrunk}\sigma T_{trunk}^4 - \sigma T_{surf}^4 \tag{55}$$

As for the 1-layer version, this radiation balance is only valid on the canopy-covered fraction of the model grid-cell, which is *(1-c_f)* for diffuse SW radiation and LW radiation, and *(1-c_f, dir)* for direct SW.

760

2.5.2 Turbulent Fluxes

Sensible heat exchange between the lower or upper canopy layer and the atmosphere is parameterized the same way as in the one-layer model version, e.g. via the resistance $r_{H,can}$. We consider that latent heat exchange between canopy and atmosphere only occurs through
765   interception evaporation and transpiration at the leaf-level, e.g. via the upper canopy layer only.

2.5.3 Biomass heat flux

The upper and lower canopy layers are respectively attributed the HM_{leaves} and HM_{trunk} heat masses from Eq. (42) and (43) which are used in the biomass heat flux parameterization (40) in the place of
770   HM_{can}.

2.5.4 Energy balance

An energy balance is formulated separately for each layer according to the energy balance equation with heat mass (Eq. (8)), where all terms are linearized as functions of T_{leaves} and T_{trunk}. The coupled
775   system is then iteratively solved for both temperatures.

The values of all the model parameters as used in the SNOWPACK canopy module are listed in Table 1.

3   Data and methods

780   3.1 Data

The data from two field sites are used here.

3.1.1 Alptal site

The first data set is from the Alptal forest site (47°03'N, 8°43'E, Erlenbach sub-catchment,
785   Switzerland ; site 1012 in the Fig. 1 of Stähli et al., 2006) that served as test-site for the SNOWMIP intercomparison study (Rutter et al., 2009) and builds on a long tradition of snow and meteorological investigations (e.g. Stähli et al., 2006; Stähli et al., 2009). The site features an ~11° west-orientated slope at 1185 m a.s.l. and is dominated by Norway spruce (85%) and silver fir (15%), with a basal area of 41 m^2 ha^{-1} and a maximum height of typically 25 m. The site LAI (including slope corrections and
790   corrections for clumping) ranges from 3.4 to 4.6 with a mean value of 3.9 m^2 m^{-2} (Stähli et al., 2009).

At this site, the SNOWPACK model is run using meteorological data derived from observations:

- Downward shortwave and longwave radiation measured on a 35 m high mast above the canopy forest. The instrument is a heated, non-ventilated CNR1 from Kipp and Zonen (2002) comprising two pyranometers CM3 (for SW) and two pyrgeometers CG3 (for LW).

26

- Precipitations measured by a heated gauge placed at 25 m height on the high mast, so that the highest trees provide a sheltering similar to a fence.

- Wind speed recorded by a cup anemometer (WMS) at 35 m on the mast.

- Air temperature measured at 35 m by a ventilated thermo-hygrometer Thygan (Meteolabor) also integrating a dew point hygrometer.

- Relative air humidity at 35 m height, derived from the air temperature and dew point.

Validation data include:

- Downward SW and LW radiation measured below the canopy (LW$\downarrow_{BC}$, SW$\downarrow_{BC}$) by a second CNR1 radiation sensor as described above, but mounted on a carrier constantly moving along a 10 m-long transect at 2 m altitude above ground at 1 m min^{-1} speed. This transect was previously shown to have a representative LAI for the stand (Stähli et al., 2009). Great care was put in the collection and pre-processing of this dataset, as below-canopy SW radiation is typically close to zero. This effort is well described in Stähli et al., 2009.

  As a post-treatment to this dataset, the LW radiation data were masked in cases when snow interception on the sensor was suspected. A typical such case is illustrated in Fig. 2: from the evening of Feb., 19th to Feb., 21st at midday, the radiation measured by the heated pyrgeometer is close to the emission level of a blackbody at 0°C (snow emissivity is around 0.98), whereas the air temperature is much colder and modelled canopy temperature closely follows the air temperature signal. The precipitation record (Fig. 2 b) features almost continuous snowfall over that period. It is hence suspected that the measured radiation originates from snow at temperature close to 0°C covering the heated pyrgeometer, and not from LW emission by the canopy. Due to their flat geometry, upwards-looking pyrgeometers are likely to remain covered by snow for substantial periods, typically a few days in alpine temperate winters. Over the 2003-2007 period, an average of 25 days per year were masked after visual identification of such events.

- Snow depth, snow density and snow water equivalent (SWE) that were measured below the canopy on a weekly basis, at 1 m intervals along a 30-m transect adjacent to the trajectory of the radiometer carrier. More details of the exact procedure are available in Stähli et al. (2009). We use the spatial average of the measurements to come up with stand-representative values.

Meteorological and validation data are available for four consecutive winter seasons between 2003 and 2007.

3.1.2 Norunda site

The second dataset is from the Norunda forest site (60°05'N, 17°28'E), located in a quite level region about 30 km north of Uppsala, Sweden, at 45 m a.s.l.. Since June 1994 it is equipped with meteorological instruments which were complemented by biomass thermometers in June and July 1995. The forest stand is composed of Scots pine (61 %), Norway spruce (34 %) and birch (5 %) with a stand LAI between 4 and 5 m^2 m^{-2}, a mean basal area of ~34.7 m^2 ha^{-1}, and a maximum tree height of ~28 m.

At this site, SNOWPACK is driven by observed meteorological variables:

- Downwelling LW and SW radiation measured by a combination of a ventilated CM21 pyranometer (Kipp and Zonen) placed at 102 m above ground at the top of a Fluxnet tower (http://fluxnet.ornl.gov/site/730) and a ventilated LXV055 net radiometer placed at 68 m on the same tower

840
- Air temperature recorded at 37 m height above ground by a copper-constantan thermocouple placed in the ventilated radiation shields

- Air humidity measured at 28 m by a HP100 TST probe (Robotronic)

- Wind speed recorded at 37 m by a sonic anemometer

845
- Precipitation data were unfortunately not available at the site. We therefore made use of precipitation data recorded at the Uppsala Aut WMO-station (WMO number: 2-462) openly provided by the Swedish Meteorological and Hydrological Institute (SMHI, http://opendata-catalog.smhi.se/explore/). This station is 26 km away from the Norunda site and the nearest station in operation at the time of the measurements used here.

The specificity of the Norunda site lies in the continuous measurement, over a summer, of the
850 biomass temperature at different heights and depths within the trunks and branches of the dominant tree species: pines and spruces. They were complemented by a detailed calculation of tree-level and stand-level biomass heat storage, which builds a unique dataset to evaluate a physics-based canopy model with heat mass. The details of the tree temperature measurements and heat storage calculations can be found in Lindroth et al. (2010).

855 In the present study we make use pine trunk temperature at 1.5 m height, which has been measured close to the trunk surface (1cm deep within the bark). Indeed, we are mostly interested in the ability of the model to reproduce the trunk surface temperature which generates the thermal emission of the trunk layer. We also provide an assessment of the canopy energy balance modelled by SNOWPACK by comparing the stand-scale modelled biomass storage flux to the one inferred from
860 observations by Lindroth et al. (2010).

3.2 Methods: Model calibration

Three versions of the canopy module, corresponding to activation of the different features of the new developments (bi-layered canopy and heat mass, Table 2), are calibrated at Alptal in order to
865 evaluate the model in its best-performance setup. Calibration is performed against the observed incoming longwave and shortwave radiation below the canopy (LW$\downarrow_{BC}$, SW$\downarrow_{BC}$). The former is specifically affected by our new developments. The observed sub-canopy SWE is not used for calibration because known uncertainties in the snowpack modelling (in link with mixed precipitation data, the treatment of rain-on-snow events and the parameterization of interception) could
870 compromise a proper calibration of the canopy module.

Depending on the version, one or two model parameters are calibrated, consistently with our modelling choices: k_{LAI} and/or f_{LAI} (Table 2).

Canopy heat mass also affects the LW radiation downwelling to the ground surface. Heat mass is a physical property of a forest stand, and not a free parameter of the model. However, its value is
875 difficult to measure and our model only proposes a coarse estimation of it (see Sect. 2). In each of the versions with heat mass, we therefore try to optimize its value considering it as an additional calibration parameter (versions 1LHM* and 2LHM*, Table 2). This procedure is designed to assess

the physical consistency of our formulation, by comparing its performance to results obtained with unrealistic heat mass values.

880 Calibration is performed by minimizing the error function CC which is the sum of the model-to-data RMSE (Root Mean Square Error) and MB (Mean Bias) for the two observed variables $LW\downarrow_{BC}$, $SW\downarrow_{BC}$.

$CC=|MB(LW\downarrow_{BC})|+|MB(SW\downarrow_{BC}|+RMSE(LW\downarrow_{BC})+RMSE(SW\downarrow_{BC})$

We prefer CC to the more common Nash-Sutcliff efficiency (NSE) because $LW\downarrow_{BC}$ and $SW\downarrow_{BC}$ exhibit a strong diurnal cycle: for such cyclic variables, even a low-performance representation of the cycles
885 yields a high NSE, and the NSE sensitivity to further improvements is typically low (Schaefli and Gupta, 2007).

4   Results

4.1 Alptal

4.1.1 Model calibration

Table 3 summarizes the results of the calibration of the five model versions (1LnoHM, 1LHM, 2LHM, 1LHM*, 2LHM*) against LW$\downarrow_{BC}$ and SW$\downarrow_{BC}$ data from the snow season 2003-2004.

For all versions, the calibrated extinction coefficient k_{LAI} is within the [0.4-0.8] range of expected values (Stähli et al., 2009). Both LW$\downarrow_{BC}$ and SW$\downarrow_{BC}$ are affected by k_{LAI}, but LW$\downarrow_{BC}$ is less sensitive to radiation extinction (as atmospheric LW extinction by canopy is partly compensated by canopy thermal emission in the same range of magnitudes). k_{LAI} is therefore mostly determined by calibration against SW$\downarrow_{BC}$ and is the same for most versions, which differ only in their modelling of LW$\downarrow_{BC}$.

The calibration of the f_{LAI} parameter partitioning *LAI* between the uppermost and lowermost canopy layers in the 2LHM version also yields the reasonable value of 0.5: this would have been an intuitive first choice for partitioning a canopy into two layers.

The successive addition of heat mass (1LHM) and a two-layer partition in the canopy (2LHM) to the default 1LnoHM simulation improves the general model performance, as reflected in the decrease of the CC error function and its components (MB, RMSE).

In the two versions where canopy heat mass is optimized (1LHM*, 2LHM*), optimization yields unrealistically high heat mass values (HM=90 kg m^{-2} and HM=60 kg m^{-2} respectively, whereby field data indicate 30 kg m^{-2}). However, while optimizing heat mass quite significantly improves the performance of the 1-layer versions (from CC=23.6 W m^{-2} for 1LHM to CC=19.3 W m^{-2} for 1LHM*), it only marginally affects the performance of the 2-layer version (from CC=18.4 W m^{-2} for 2LHM to CC=17.5 W m^{-2} for 2LnoHM). These are encouraging results for the 2-layer canopy formulation: on the one hand, this model version shows a better performance than the one-layered canopy model, even with the physically-estimated heat mass. With the one-layered version such a performance can only be approached with an unrealistic canopy heat mass. On the other hand, the performance of 2LHM shows a considerably reduced sensitivity to the prescribed areal heat mass of the canopy, a physical parameter which can be spatially variable and hard to retrieve with precision over non-investigated forested areas.

For the two snow seasons when all model versions simulate a reasonable dynamics for the Alptal snowpack (2004-2005 and 2006-2007, see Sect. 4.1.3), the sensitivity of the modeled SWE to the calibration parameters k_{LAI} and f_{LAI} was determined (not shown). The modeled SWE is sensitive to k_{LAI} and f_{LAI}, but the calibrated (k_{LAI}, f_{LAI}) values lead to RMSE to observed SWE close to the absolute minimum obtained when variing k_{LAI} and f_{LAI} over their full range (13 mm vs 10 mm at minimum for 2006-2007). In the surrounding of the calibrated (k_{LAI}, f_{LAI}) values, the modelled SWE has furthermore a reduced sensitivity to variations in k_{LAI} and f_{LAI}. This result enhances our confidence in the model robustness.

The performance of all model versions after calibration over 2003-2004 slightly degrades over the longer 2003-2007 time-period when observations are available. Especially the MB in LW$\downarrow_{BC}$, and (to a

smaller degree) in SW$\downarrow_{BC}$, are increased over 2003-2007, questioning the transferability of our 2003-2004 calibration. We therefore calibrate the 1LnoHM, 1LHM and 2LHM versions over the 2003-2007 period and analyse the changes in best-fit parameters and performance (Table 4).

The calibration over 2003-2007 yields a slightly different best-fit parameter value for the extinction coefficient in the 1LHM and 2LHM versions (k_{LAI} = 0.85 vs k_{LAI} =0.75 when calibrated over 2003-2004): this enhanced radiation extinction improves the MB for SW$\downarrow_{BC}$ over the 2003-2007 period, but slightly degrades the results over 2003-2004. The overall picture is however not changed upon this new calibration:

- over both periods, 2LHM performs better than 1LHM which also performs better than 1LnoHM: this is an indication of the added value of our new parameterizations.

- for all model versions, performance is better over 2003-2004 than over the full 2003-2007 period, especially for LW$\downarrow_{BC}$. This may indicate that our model is still too simple to capture the full range of snow-forest processes.

- over both periods, the two, slightly different calibrations yield thoroughly comparable model performances. This gives confidence in the validity of our calibration and in the possibility of calibrating the model over only one year of data.

In the simulations discussed in the rest of the paper, calibration over 2003-2007 is used.

4.1.2 Model evaluation against thermal radiation

In Fig. 3 are compared observed and modelled LW$\downarrow_{BC}$ as computed by the different model versions without heat mass optimization (1LnoHM, 1LHM, 2LHM) over the 2003-2004 calibration period. Similarly to the performance metrics of Table 3, it illustrates gradually increasing model performances from the 1LnoHM to the 2LHM model versions.

With respect to 1LnoHM, the consideration of the trees heat mass in 1LHM slightly delays and reduces the canopy cooling at night and warming up in the morning: this translates into a slight delay and smoothing of the diurnal cycle of LW$\downarrow_{BC}$, part of which originates from canopy thermal emission.

More striking, however, is the attenuation of the daily amplitude of LW$\downarrow_{BC}$ induced by 2LHM, which brings the modelling results in closer agreement to observations: especially, the night-time (6PM-6AM) mean bias in LW$\downarrow_{BC}$ is considerably reduced in 2LHM with respect to other model versions, amounting to -10.8, -7.8 and -2.8 W m^{-2} in 1LnoHM, 1LHm and 2LHM respectively.

When only one bulk layer of canopy is considered, this layer is exposed at night to intense radiative cooling towards the sky, whose thermal emissivity is low. With two layers of canopy, only the uppermost layer experiences this uncompensated cooling. The lower layer receives thermal radiation from the upper layer which has a higher emissivity than the sky. This thermal sheltering yields higher temperature and LW emission at night from the lower canopy towards the ground surface. This mechanism proves to efficiently reproduce the daily cycles (Fig. 3 a, b) and daily averages (Fig. 3 c) of the thermal radiation affecting the snowpack.

4.1.3 Impact on the underlying snowpack

Over the four winters of interest here, a similar ranking of sub-canopy SWE modelled by 1LnoHM,
970   1LHM and 2LHM is observed, with 1LHM accumulating most snow and 2LHM generally featuring the
smallest SWE (except for the 2005-2006 winter; Fig. 3 c and 4). With respect to the thermal behaviors
of the different model versions, such a result is somehow counter-intuitive as 1LHM and 2LHM
generally deliver greater amounts of LW radiation to the snowpack than does 1LnoHM (Fig. 3 c.),
hence contributing more energy to mid-winter ablation events (e.g. Fig. 3 d., December to January).
975   In 1LHM, this increased ablation is, however, compensated by a different effect of the thermal
canopy mass: as a result of the high thermal mass of the bulk canopy in 1LHM, the canopy
temperature and hence interception evaporation is reduced, and more snow unloads than in the two
other versions, resulting in higher sub-canopy snow accumulation. In 2LHM, the high diurnal
temperature variations of the upper canopy temperature combine with stronger LW radiation to the
980   snowpack, resulting in a thinner snowpack.

Noteworthy, the model ability to represent SWE (as typically assessed by the RMSE to observations)
is degraded in 1LHM and improved in 2LHM with respect to the original canopy module 1LnoHM. The
LW-enhanced ablation in 2LHM (and small associated changes in interception evaporation) does
therefore not deteriorate the overall model skills.

985   In some specific ablation periods, 2LHM also proves to reproduce the observed snowpack dynamics
better: one such event is the early February 2004 severe ablation, when high thermal exposure of the
snowpack is better reproduced by 2LHM (Fig. 3 c) while the concomitant ablation is also stronger in
2LHM, which matches the observations better (Fig. 3 d). Similarly, the LW-enhanced ablation in
2LHM leads to a sub-canopy SWE dynamics in closer agreement with observations in the 2005
990   ablation phase and in early 2007 (mid-winter complete snow disappearance).

As mentioned in the methods, we do not trust the modeling of the accumulation phases, where high
uncertainties in precipitation phase and interception (enhanced by the warm temperatures at Alptal)
can initiate a permanent bias in the modeled snow cover. Therefore, we do not use observed SWE
records to validate or evaluate our model. However, the capability of a model to better reproduce
995   observed, relative ablation events where precipitations are absent (like in the 2005 main ablation
phase) reliably means enhanced performances: our results are therefore encouraging for the overall
consistency of the 2LHM canopy module.

4.2 Norunda: tree temperature and biomass storage flux

1000   At the Norunda site, SNOWPACK is run using the Alptal calibration from 2003-2007, and a canopy
basal area and areal heat mass derived from local data (Sect. 3). The difference in latitudes (hence in
solar angle), tree species (mostly Scots Pine at Norunda) and context (Alpine winter vs boreal
summer) between both sites constitutes a huge challenge and an excellent benchmark to test one
desired feature of a physically-based model, e.g. its transferability to different climate and ecosystem
1005   types. We here specify that SNOWPACK includes all the necessary features to be used as a Soil-
Vegetation-Atmosphere-Transfer model (SVAT) in the absence of a snow cover: a soil water balance,
a surface and canopy energy balance, and a temperature diffusion scheme in the soil. The model has
also been used as such in continuous multi-year simulations in previous studies (e.g. Bavay et al.,
2013).

1010   We compare observed tree trunk temperature to modelled temperature of the bulk canopy (for 1LnoHM and 1LHM) or of the lower trunk layer (for 2LHM) over summer 1995 at Norunda (Fig. 5, Table 5). The modelled trunk layer temperature of 2LHM shows an improved ability to reproduce the observed tree trunk temperature signal: similiar to the improvements seen at Alptal, radiative loss of energy from the lower layer at night is considerably reduced with 2LHM, bringing night-time

1015   modelled temperature in closer agreement to observed data at Norunda. Also, the reduced SW insolation received by the lower canopy layer during daytime in 2LHM prevents too high mid-day temperature of the trunks, an observation that 1LHM and 1LnoHM cannot reproduce. Finally, the combination of thermal sheltering of the lowermost canopy layer and its thermal inertia delays the tree trunk cooling (resp. warming) at evening (resp. morning) times, improving the temporal

1020   correlation with observations.

Heat fluxes to canopy elements are a substantial, though not dominant, component of the canopy energy balance (Lindroth et al., 2010, their Fig. 6): they can amount to ~7% of the daily net radiation received by the canopy. To assess the consistency of the SNOWPACK canopy module we compare the modelled canopy heat fluxes to the ones derived by Lindroth et al. (2010) from field measurements

1025   and extrapolated at the stand scale. Note that 1LnoHM, having no heat mass, does not consider any such fluxes.

Both the 1LHM and 2LHM versions overestimate the daily amplitude of biomass heat fluxes with respect to observations, with an increased bias for 1LHM (Fig. 6; Table 5). This is in line with an overestimation of the daily amplitude of canopy temperature (or of the temperature of the lower

1030   canopy layer for 2LHM) which is stronger with 1LHM (Fig. 5). Also, the model biomass heat fluxes peak ~2h earlier than the observed ones. We interpret this as an artefact of modelling the canopy with only one or two thermally homogeneous layers, whereas it is in reality a continuous medium experiencing thermal diffusion at scales smaller than our layers. In reality, the low thermal inertia of a bark surface layer provokes quick surface heating as a result of solar energy input (e.g. in the

1035   morning). This temporarily limits further heating from turbulent and radiative fluxes, until the surface heat has diffused into the trunk. In other words, heat uptake by trunks is diffusion limited. Contrarily, the bulk, thermally inert trunk layer of our model heats up to a smaller temperature because the heat flux is accommodated by the whole layer and not only by its uppermost surface: further heating by turbulent and radiative fluxes is then still possible and the heat flux towards the biomass keeps

1040   being sustained. As a result, our modelled canopy accommodates incoming energy more rapidly than a real one during the first part of the diurnal cycle. The aforementioned mechanism can also cause the accommodation of more heat energy by the modeled trunk layer than in reality: in reality, the capacity of the canopy to accommodate heat is limited by thermal diffusion within the wood. Heat uptake stops when available solar energy starts going down. At that time, the wooden medium may

1045   not have reached an homogeneous, high temperature yet (e.g. Fig. 1 from Lindroth et al., 2010).

As such, the representation of the biomass storage fluxes by 1LHM and 2LHM yield only moderate improvement to the model: they feature a reasonable (though slightly shifted) diurnal cycle (cf. the correlation coefficients in Table 5) but their RMSE to observations is of the order of magnitude of the standard deviation of the observed biomass fluxes (Table 5, first row).

1050   However, model performance, especially for 2LHM, is improved if the total heat storage flux towards the biomass and canopy air space is considered (thick black line in Fig. 6, Table 5). The air heat storage flux corresponds to the changes in latent and sensible heat stored in the within-canopy air

space. Lindroth et al. (2010) provide estimates of these heat storage terms based on air temperature and humidity measurements at 7 heights within the canopy air space. On a daily basis, the air heat storage term reacts more rapidly to solar heating than the biomass heat storage flux. The air heat storage flux is not specifically accounted for in SNOWPACK. However, the increased correlation coefficient and reduced RMSE obtained when the SNOWPACK canopy heat flux is compared to the sum of estimated air and biomass heat fluxes, indicate that the canopy module produces a bulk representation of the observed fluxes. Such a result should be confirmed against further observational datasets.

5   Discussion

Our results show that the new features implemented in the SNOWPACK canopy module, especially the two-layer scheme, improve the representation of the radiation budget at the sub-canopy level. The importance of accounting for the canopy temperature and for contrasts between different canopy elements has often been underlined (Sicart et al., 2004; Pomeroy et al., 2009). Pomeroy et al. (2009) compared three sub-canopy thermal irradiance models based on measurements of (i) air temperature only; (ii) air, trunk and needles temperatures and (iii) air temperature and empirical shortwave-to-longwave conversion function by the canopy. The two latter formulations exhibited distinctively better performances than the first one in terms of mean bias and RMSE in both the uniform and discontinuous stands investigated. Our present work confirms these findings but also proposes a seamless physics-based canopy model to account for this effect. This has to our knowledge never been brought to the scientific literature.

Radiation can be an important driver of the spring-time sub-canopy snow energy balance and subsequent melt. Garvelmann et al. (2014) report a contribution of about 50% from the net longwave radiation to the sub-canopy energy balance during two cloudy-sky rain-on-snow events closely monitored in the Black Forest, Germany. In open environments the longwave contribution to the surface energy balance does not exceed 20% for the same meteorological conditions, and is at times negative. According to Lundquist et al. (2013), forest regions with average December-January-February (DJF) temperatures greater than -1°C experience 1 to 2 weeks reduction in snow-cover duration compared to adjacent open areas because of increasing longwave radiation from the canopies. There, the sub-canopy snowpack is mostly impacted during mid-winter warm events, when the longwave enhancement by the canopy dominates over the shadowing from shortwave radiations. This is precisely the situation observed at Alptal, where mean DJF temperature is about 1.5°C (1975-2005), and our improved canopy module with more realistic thermal heating from the canopy yields a better reproduction of the two mid-winter ablation events from 2004-2005 and 2006-2007. In that sense our work contributes an enhanced capability at modelling sub-canopy melt conditions that can jointly benefit water and forest management (Lawler and Link, 2011 ; Ellis et al., 2013).

In line with Rutter et al. (2009), Essery et al. (2008), and many others, we agree that the mass balance of snow is most relevant when it comes to snow hydrological applications or to the assessment of snow hazards. In the forest, snow interception and subsequent sublimation of intercepted snow majorly affects the sub-canopy mass balance: reductions up to 60% for sub-canopy snowfall have been reported as a result of these processes (Hardy et al., 1997). Radiation, as the main driver of the melt, shapes the end-of-season snow mass-balance, but the latter also critically depends on peak accumulation from the accumulation phase which our developments barely touch. We see our contribution as a necessary step in a sequential, multi-directional validation process, whereby the careful and independent validation of each component of the snow model will gradually improve its skills: SNOWPACK being now equipped with a more reliable and sophisticated radiative transfer scheme for the canopy, diagnosing flaws originating from other processes (mixed-precipitations, rain-on-snow events or misrepresented canopy interception) should be easier. Promising work has just been published very recently as to new ways to parameterize canopy interception in alpine forests (Moeser et al., 2015). The proposed methodology should later serve the

improvement of snow models like SNOWPACK in aspects of crucial interest for the snow mass balance.

Other physical processes could further improve SNOWPACK: in the present version the within-canopy air humidity is equal to the above-canopy one, while Durot (1999) show a 10 to 20% increase in within-canopy air humidity in spring, with peaks during unloading. This should impact the modeled sub-canopy turbulent and radiative fluxes. Also, the reduction of albedo as a result of canopy debris should be considered, though tests performed at Alptal didn't show much change upon a specific parameterization of sub-canopy snow ageing.

Further wintertime assessment of model performance in colder, controlled environments, where mixed precipitation events are scarce but radiation play an important role, would help confirm the added value of our new canopy formulation for the representation of sub-canopy snow dynamics. Data from the SnowMIP sites could be used for that purpose provided they are combined with site knowledge and expertise, and ancillary data that help fit important model parameters to the local canopy conditions (interception, radiation extinction).

SNOWPACK has a multi-layer and detailed representation of snow and soil, which features a highly resolved modelling of energy and mass balance in thin layers including e.g. snow metamorphism and freezing point depressions during phase change in soil (Wever et al., 2014). This detailed and physics-based description should have a corresponding representation of canopy processes, which has not been the case in earlier versions of SNOWPACK. The more detailed model described in this contribution is therefore a consistent extension of SNOWPACK and leads to an overall more balanced representation of processes in the air - canopy - snow - soil continuum. A physics-based, integrated modelling chain featuring such level of homogeneity and detail is rare. **Sivapalan et al. (2003) and Rutter et al. (2009) underlined that such process-based model (rather than calibration of parametric models) offer the best possibility to address the current hydrological and ecosystemic challenges related to snow in a manner that ensures site-transferability and robustness with respect to changing climate. The new version of SNOWPACK with the 2-layer canopy module b**uilds a sound basis for such investigations. The current two-layer formulation of the canopy is also a suitable basis for a future model adaptation to deciduous forest environments.

Our two-layer canopy model exhibits robustness in two ways:

- First, it shows little sensitivity to physical parameters that are hard to assess from standard forestry metrics or for non-investigated forests. The canopy heat mass is one of such parameters, as stated in Sect. 4. The other one is the fraction of LAI attributed to the top-most ("leafy") canopy layer, as illustrated in Fig. 7. The ratio of woody to total plant area is hard to measure optically, especially for evergreen canopies (Weiss et al., 2004). Pomeroy et al. (2009) used a formulation somewhat similar to ours to attribute LW radiation to emission from leafy or woody elements. They conclude that, depending on the forest structure and type, the needle-branch fraction as seen from a ground observer would range from 0.6 to 0.75 of the total plant elements. Our Alptal calibration attributing 50% of canopy LAI to the uppermost, leaf-only layer is consistent with this model-based estimate for leaf and branches.

- Second, the model exhibits a good performance at the Norunda site, while its free parameters (k_{LAI} and f_{LAI}) have been calibrated in a different forest ecosystem and climatic

context at Alptal. In both forests, coniferous species are dominant and it is suspected that extrapolation of our parameterizations to deciduous forests requires further adaptation. However, our results give confidence in the possibility of using our physics-based model without prior tuning in different alpine and sub-arctic catchments majorly covered by conifers.

Finally, it is a quite general finding that two-layer formulations of physical continuums often bring substantial improvements over single-layer ones. The step from big-leaf soil-vegetation-atmosphere transfer models to dual-source models (e.g. Blyth et al., 1999; Bewley et al., 2010) is a typically illustration of this phenomenon for the computation of the land surface energy balance. Similarly, Dai et al. (2004) improved their modelling of forest CO_2 absorption by considering different regimes for sunlit and shaded leaves. Our results here are in line with this more general observation.

6   Conclusion

Our new canopy model demonstrates ability to simulate the difference in the thermal regimes of the canopy leafy and woody compartments, as assessed by comparison to observed canopy temperature and thermal radiation. This is achieved via the separation of the canopy in two layers of different heat masses, radiatively interacting with each other. In comparison, a one-layered version of the canopy module always yields poorer results despite optimization attempts. The most striking improvement is the reduction in night-time canopy cold bias, which can only be achieved via the two-layer formulation and results from the sheltering role of the upper canopy layer.

The robustness of the new canopy model is confirmed by the successful evaluation of the model without prior tuning at a boreal, coniferous site. The new formulation besides shows a weak sensitivity to biomass areal heat mass, a forest-dependent input parameter that can be hard to estimate locally. Model evaluation against snow water equivalent data indicate that the new parameterizations do not degrade the overall model skills while improving the representation of some LW-enhanced ablation events.

The improved representation of the radiative components of the sub-canopy energy balance achieved here opens the path to the tracking, understanding and modelling of further processes relevant for the underlying snowpack like turbulent fluxes or heat advection by rain. In the end, enhanced models and process understanding should help obtain better hydrological simulation tools for crucial purposes like climate change impact assessment.

References

ACIA: Arctic Climate Impact Assessment, Cambridge University Press, URL http://www.acia.uaf.edu, 2005.

Adams, R., Spittlehouse, D., and Winkler, R.: The e_ect of a canopy on the snowmelt energy balance, in: Proceedings of the 64th Annual Meeting Western Snow Conference, pp. 171–174, 1996.

Axelsson, B. and Agren, G.: Tree growth model (PT 1) a development paper, Swedish Coniferous Forest Project Internal Report, 1976.

Bartelt, P. and Lehning, M.: A physical SNOWPACK model for the Swiss avalanche warning: Part I: numerical model, Cold Reg. Sci. Technol., 35, 123–145, 2002.

Bavay, M., Grunewald, M., Lehning, M.: Response of snow cover and runoff to climate change in high Alpine catchments of Eastern Switzerland. Adv. Water Resour., 55, 4–16, 2013.

Bavay, M. and Egger, T.: MeteoIO 2.4.2: a preprocessing library for meteorological data, Geosci. Model Dev., 7, 3135-3151, doi:10.5194/gmd-7-3135-2014, 2014.

Beljaars, A. and Holtslag, A.: Flux parameterization over land surfaces for atmospheric models, J. Appl. Meteorol., 30, 327–341, 1991.

Bewley, D., Essery, R., Pomeroy, J., and M_enard, C.: Measurements and modelling of snowmelt and turbulent heat fluxes over shrub tundra, Hydrol. Earth Syst. Sci., 14, 1331–1340, 2010.

Blyth, E., Harding, R., and Essery, R.: A coupled dual source GCM SVAT, Hydrol. Earth Syst. Sci., 3, 71–84, 1999.

Chen, J. M., Rich, P. M., Gower, S. T., Norman, J. M., and Plummer, S.: Leaf area index of boreal forests: Theory, techniques, and measurements, J. Geophys. Res. Atmospheres (1984–2012)., 102, 29 429–29 443, 1997.

Comola, F., Schaefli, B., Rinaldo, A., and Lehning, M.: Thermodynamics in the hydrologic response: Travel time formulation and application to Alpine catchments. Water Resources Research, 51(3), 1671-1687, 2015.

Dai, Y., Dickinson, R. E., and Wang, Y.-P.: A two-big-leaf model for canopy temperature, photosynthesis, and stomatal conductance, J. Clim., 17, 2281–2299, 2004.

Durot, K. Modélisation hydrologique distribuée du bassin versant pluvio-nival de Sarennes. Validation des données d'entrée et développement d'un module de fonte nivale sous foret (in French). PhD thesis, Institut National Polytechnique de Grenoble, Grenoble, 1999.

Ellis, C., Pomeroy, J. and Link, T.: Modeling increases in snowmelt yield and desynchronization resulting from forest gap-thinning treatments in a northern mountain headwater basin. Wat. Resour. Res., 49, 1–14, doi:10.1002/wrcr.20089, 2013.

Erbs, D., Klein, S., and Duffie, J.: Estimation of the diffuse radiation fraction for hourly, daily and monthly-average global radiation, Sol. Energy., 28, 293–302, 1982.

Essery, R.: Boreal forests and snow in climate models, Hydrol. Process., 12, 1561-1568, 1998.

1225   Essery, R., Li, L., and Pomeroy, J.: A distributed model of blowing snow over complex terrain, Hydrol. Process., 13, 2423–2438, 1999.

Essery, R., Pomeroy, J., Parviainen, J., and Storck, P.: Sublimation of snow from coniferous forests in a climate model, J. Clim., 16, 1855–1864, 2003.

Essery, R., Rutter, N., Pomeroy, J., Baxter, R., Stähli, M., Gustafsson, D., Barr, A., Bartlett, P., and
1230   Elder, K.: SnowMIP2: an evaluation of forest snow process simulation, Bull. Am. Meteorol. Soc., 2008.

Etchevers, P., Martin, E., Brown, R., Fierz, C., Lejeune, Y., Bazile, E., Boone, A., Dai, Y.J., Essery, R., Fernandez, A., Gusev, Y., Jordan, R., Koren, V., Kowalczyk, E., Nasonova, N.O., Pyles, R.D., Schlosser, A., Shmakin, A.B., Smirnova, T.G., Strasser, U., Verseghy, D., Yamazaki, T., Yang, Z-L.: Validation of the energy budget of an alpine snowpack simulated by several snow models (SnowMIP project).
1235   Annals Glaciol., 38, 150-158, 2004.

Garvelmann, J., Pohl, S., and Weiler, M.: Variability of observed energy fluxes during rain-on-snow and clear sky snowmelt in a mid-latitude mountain environment, J. Hydrometeorol., 2014.

Gouttevin, I., Menegoz, M., Dominé, F., Krinner, G., Koven, C., Ciais, P., Tarnocai, C., and Boike, J.: How the insulating properties of snow affect soil carbon distribution in the continental pan-Arctic
1240   area, J. Geophys. Res., 117, G02 020, 2012.

Grippa, M., Kergoat, L., Le Toan, T., Mognard, N., Delbart, N., L'Hermitte, J., and Vicente-Serrano, S.: The impact of snow depth and snowmelt on the vegetation variability over central Siberia, Geophys. Res. Lett., 32, 2005.

Groot Zwaaftink, C. D., Loewe, H., Mott, R., Bavay, M. and Lehning, M.: Drifting snow sublimation: A
1245   high-resolution 3-D model with temperature and moisture feedbacks. J. Geophys. Res. Atmospheres, 116, D16107, 1984–2012, **doi:10.1029/2011JD015754**, 2011.

Gryning, S.-E., Batchvarova, E., and De Bruin, H.: Energy balance of a sparse coniferous high-latitude forest under winter conditions, Boundary-Layer Meteorol., 99, 465–488, 2001.

Gustafsson, J., Brooks, P., Molotch, N., and Veatch, W.: Estimating snow sublimation using natural
1250   chemical and isotopic tracers across a gradient of solar radiation, Water Resour. Res., 46, W12511, 2010.

Harding, R. and Pomeroy, J.: The energy balance of the winter boreal landscape, J. Clim., 9, 2778–2787, 1996.

Hardy, J., Davis, R., Jordan, R., Li, X., Woodcock, C., Ni, W., and McKenzie, J.: Snow ablation modeling
1255   at the stand scale in a boreal jack pine forest, J. Geophys. Res. Atmospheres (1984–2012)., 102, 29 397–29 405, 1997.

Hedstrom, N. and Pomeroy, J.: Measurements and modelling of snow interception in the boreal forest, Hydrol. Process., 12, 1611–1625, 1998.

Helbig, N., Löwe, H., and Lehning, M.: Radiosity approach for the shortwave surface radiation balance in complex terrain, J. Atmospheric Sci., 66, 2900–2912, 2009.

Hogstrom, U.: Review of some basic characteristics of the atmospheric surface layer, in: Boundary-Layer Meteorology 25th Anniversary Volume, 1970–1995, pp. 215–246, Springer, 1996.

Jansson, P. and Karlberg, L.: Coupled heat and mass transfer model for soil–plant–atmosphere systems. TRITA-AMI report 30 87, Royal Institute of Technology, Department of Civil and Environmental Engineering, Stockholm, 435 pp, 2001.

Jarvis, P.: The interpretation of the variations in leaf water potential and stomatal conductance found in canopies in the field, Philos. Transactions Royal Soc. Lond., 273, 593–610, 1976.

Kavetski, D. and Kuczera, G.: Model smoothing strategies to remove microscale discontinuities and spurious secondary optima in objective functions in hydrological calibration, Water resources research., 43, 2007.

Kelley Jr, J., Weaver, D., and Smith, B.: The variation of carbon dioxide under the snow in the Arctic, Ecol., pp. 358–361, 1968.

Kipp and Zonen: Instruction manual to the CNR1 Net Radiometer, 2002.

Koivusalo, H. and Kokkonen, T.: Snow processes in a forest clearing and in a coniferous forest, J. Hydrol., 262, 145–164, 2002.

Lawler, R.R. and Link, T.E.: Quantification of incoming all-wave radiation in discontinuous forest canopies with application to snowmelt prediction. Hydrol. Process., 25, 21, doi: 10.1002/hyp.8150, 2011.

Lawrence, D. and Slater, A.: The contribution of snow condition trends to future ground climate, Clim. Dyn., 34, 969–981, 2010.

Lehning, M., Bartelt, P., Brown, B., and Fierz, C.: A physical SNOWPACK model for the Swiss avalanche warning: Part III: Meteorological forcing, thin layer formation and evaluation, Cold Reg. Sci. Technol., 35, 169–184, 2002a.

Lehning, M., Bartelt, P., Brown, B., Fierz, C., and Satyawali, P.: A physical SNOWPACK model for the Swiss avalanche warning: Part II. Snow microstructure, Cold Reg. Sci. Technol., 35, 147–167, 2002b.

Lehning, M., Völksch, I., Gustafsson, D., Nguyen, T. A., Steahli, M., and Zappa, M.: ALPINE3D: a detailed model of mountain surface processes and its application to snow hydrology, Hydrol. Process., 20, 2111–2128, 2006.

Lehning, M., Löwe, H., Ryser, M., and Raderschall, N.: Inhomogeneous precipitation distribution and snow transport in steep terrain, Water Resour. Res., 44, 2008.

Lindroth, A., Mölder, M., and Lagergren, F.: Heat storage in forest biomass improves energy balance closure, Biogeosciences., 7, 301–313, 2010.

Liston, G. and Elder, K.: A Distributed Snow-Evolution Modeling System (SnowModel). J. of Hydrometeorol., 7, 1259-1276, 2006.

1295   Liston, G., Mcfadden, J., Sturm, M., and Pielke, R.: Modelled changes in arctic tundra snow, energy and moisture fluxes due to increased shrubs, Glob. Chang. Biol., 8, 17–32, 2002.

Lundberg, A., Calder, I., and Harding, R.: Evaporation of intercepted snow: measurement and modelling, J. Hydrol., 206, 151–163, 1998.

Lundquist, J. D., Dickerson-Lange, S. E., Lutz, J. A., and Cristea, N. C.: Lower forest density enhances
1300   snow retention in regions with warmer winters: A global framework developed from plot-scale observations and modeling, Water Resour. Res., 49, 6356–6370, 2013.

Mellander, P.-E., Stähli, M., Gustafsson, D., and Bishop, K.: Modelling the effect of low soil temperatures on transpiration by Scots pine, Hydrol. Process., 20, 1929–1944, 2006.

Merriam, R. A.: A note on the interception loss equation, J. Geophys. Res.., 65, 3850–3851, **1960.**

1305   **Moeser, D.,** Stähli**, M. and Jonas, T. :** **Improved snow interception modeling using canopy** parameters derived from airborne LIDAR data. Wat. Resour. Res., Accepted Article, doi: 10.1002/2014WR016724, 2015.

Musselman, K. N., Molotch, N. P., Margulis, S. A., Lehning, M., and Gustafsson, D.: Improved snowmelt simulations with a canopy model forced with photo-derived direct beam canopy
1310   transmissivity, Water Resour. Res., 48, 2012.

Nash, J. and Sutcliffe, J.: River flow forecasting through conceptual models part IA discussion of principles, J. Hydrol.., 10, 282–290, 1970.

Otterman, J., Staenz, K., Itten, K., and Kukla, G.: Dependence of snow melting and surface-atmosphere interactions on the forest structure, Boundary-Layer Meteorol., 45, 1–8, 1988.

1315   Pomeroy, J. W. and Essery, R.: Turbulent fluxes during blowing snow: field tests of model sublimation predictions, Hydrol. Process., 13, 2963–2975, 1999.

Pomeroy, J. W., Parviainen, J., Hedstrom, N., and Gray, D.: Coupled modelling of forest snow interception and sublimation, Hydrol. Process., 12, 2317–2337, 1998.

Pomeroy, J. W., Gray, D., Hedstrom, N., and Janowicz, J.: Prediction of seasonal snow accumulation in
1320   cold climate forests, Hydrol. Process., 16, 3543–3558, 2002.

Pomeroy, J. W., Marks, D., Link, T., Ellis, C., Hardy, J., Rowlands, A., and Granger, R.: The impact of coniferous forest temperature on incoming longwave radiation to melting snow, Hydrol. Process., 23, 2513–2525, 2009.

Rasmus, S., Grönholm, T., Lehning, M., Rasmus, K., and Kulmala, M.: Validation of the SNOWPACK
1325   model in five different snow zones in Finland, Boreal Environ. Res., 12, 467–488, 2007.

Rasmus, S., Lundell, R., and Saarinen, T.: Interactions between snow, canopy, and vegetation in a boreal coniferous forest, Plant Ecology & Diversity, 4, 55–65, 2011.

Rutter, N., Essery, R., Pomeroy, J., Altimir, N., Andreadis, K., Baker, I., Barr, A., Bartlett, P., Boone, A., Deng, H., et al.: Evaluation of forest snow processes models (SnowMIP2), J. Geophys. Res. Atmospheres (1984–2012)., 114, 2009.

Saccone, P., Morin, S., Baptist, F., Bonneville, J.-M., Colace, M.-P., Domine, F., Faure, M., Geremia, R., Lochet, J., Poly, F., et al.: The effects of snowpack properties and plant strategies on litter decomposition during winter in subalpine meadows, Plant Soil., 363, 215–229, 2013.

Schaeffli, B. and Gupta, H. V.: Do Nash values have value?, Hydrol. Process., 21, 2075–2080, 2007.

Schmidt, R. and Gluns, D. R.: Snowfall interception on branches of three conifer species, Can. J. For. Res., 21, 1262–1269, 1991.

Shuttleworth, W. J. and Wallace, J.: Evaporation from sparse crops-an energy combination theory, Q. J. Royal Meteorol. Soc., 111, 839–855, 1985.

Sicart, J. E., Essery, R. L., Pomeroy, J. W., Hardy, J., Link, T., and Marks, D.: A sensitivity study of daytime net radiation during snowmelt to forest canopy and atmospheric conditions, J. Hydrometeorol., 5, 774–784, 2004.

Sivapalan, M., Takeuchi, K., Franks, S., Gupta, V., Karambiri, H., Lakshmi, V., Liang, X., McDonnell, J., Mendiondo, E., O'connell, P., et al.: IAHS Decade on Predictions in Ungauged Basins (PUB), 2003–2012: Shaping an exciting future for the hydrological sciences, Hydrol. Sci. J., 48, 857–880, 2003.

Stähli, M. and Gustafsson, D.: Long-term investigations of the snow cover in a subalpine semi-forested catchment, Hydrol. Process.., 20, 411–428, 2006.

Stähli, M., Jonas, T., and Gustafsson, D.: The role of snow interception in winter-time radiation processes of a coniferous sub-alpine forest, Hydrol. Process., 23, 2498–2512, 2009.

Strasser, U., Warscher, M., and Liston, G. E.: Modeling snow-canopy processes on an idealized mountain, J. Hydrometeorol., 12, 663–677, 2011.

Taconet, O., Bernard, R., and Vidal-Madjar, D.: Evapotranspiration over an agricultural region using a surface flux/temperature model based on NOAA-AVHRR data, J. Clim. Appl. Meteorol., 25, 284–307, 1986.

Tribbeck, M., Gurney, R., and Morris, E.: The radiative effect of a fir canopy on a snowpack, J. Hydrometeorol., 7, 880–895, 2006.

Tribbeck, M. J., Gurney, R. J., Morris, E. M., and Pearson, D. W.: A new Snow-SVAT to simulate the accumulation and ablation of seasonal snow cover beneath a forest canopy, J. Glaciol., 50, 171–182, 2004.

Tyler, N.: Climate, snow, ice, crashes, and declines in populations of reindeer and caribou (Rangifer tarandus L.), Ecol. Monogr., 80, 197–219, 2010.

Vikhamar-Schuler, D., Hanssen-Bauer, I., Schuler, T., Mathiesen, S., and Lehning, M.: Use of a multilayer snow model to assess grazing conditions for reindeer, Annals Glaciol., 54, 214–226, 2013.

Weiss, M., Baret, F., Smith, G., Jonckheere, I., and Coppin, P.: Review of methods for in situ leaf area index (LAI) determination: Part II. Estimation of LAI, errors and sampling, Agric. For. Meteorol., 121, 37–53, 2004.

Wever, N., Fierz, C., Mitterer, C., Hirashima, H., and Lehning, M.: Solving Richards Equation for snow improves snowpack meltwater runoff estimations in detailed multi-layer snowpack model, The Cryosphere., 8, 257–274, 2014.

Yamazaki, T.: A One-dimensional Land Surface Model Adaptable to Intensely Cold Regions and its Applications in Eastern Siberia., J. Meteorol. Soc. Jpn., 79, 1107–1118, 2001.

Yamazaki, T. and Kondo, J.: The snowmelt and heat balance in snow-covered forested areas, J. Appl. Meteorol., 31, 1322–1327, 1992.

Zappa, M., Pos, F., Strasser, U., Warmerdams, P., and Gurtz, J.: Seasonal water balance of an Alpine catchment as evaluated by different methods for spatially distributed snowmelt modelling, Nord. Hydrol., 34, 179–202, 2003.

1365

1370

1375

Tables

Table 1. Parameters used by the SNOWPACK canopy module.

	Parameter (unit)	Description	value
Model internal parameters	i_{max} (mm m^{-2})	Coefficient for the maximum interception capacity	Spruce: 5.9 Pine: 6.6
	i_{LAI} (mm m^{-2})	Maximum interception of water by canopy per unit of *LAI*	Rain: 0.25 Snow: $i_{max}(0.27+46/\rho_{s,int})$
	k_{LAI} (-)	Extinction coefficient for SW and LW radiations	[0.4 – 0.8] default: 0.75
	f_{LAI} (-)	Fraction of LAI in the uppermost canopy layer. For 2LHM only.	default: 0.5
	D_{can} (m)	Average canopy diameter	1
	$\alpha_{wet,\ snow}$ (-)	Snow-covered canopy albedo	0.3
	$\alpha_{dry} = \alpha_{wet,\ rain}$ (-)	Dry and wet canopy albedo	0.11
	α_{trunk} (-)	lower canopy layer albedo	0.09
	f_d (-)	Ratio d/z_{can}	2/3
	f_{z0m} (-)	Ratio z_{0m}/z_{can}	0.1
	$f_{z0h/z0m}$ (-)	Ratio z_{0h}/z_{0m}	0,999
	$r_{a,LAI}$ (-)	Parameter for the excess resistance introduces by canopy between surface and reference level.	3.
	$f_{ra,snow}$	Factor for increased aerodynamic resistance for evaporation of intercepted snow	10
	$\rho_{biomass}$ (kg m^{-3})	Bulk biomass density	900
	$C_{p,biomass}$ (J kg^{-1} K^{-1})	Bulk biomass heat capacity	2800
	e_{leaf} (m)	Mean leaf (or needle) thickness. For 2LHM only.	0.001
User-provided	z_{can} (m)	Mean canopy height	
	LAI (m^2 m^{-2})	One-sided mean stand leaf-area index	
	cf (-)	Direct throughfall fraction	

B (m^2 m^{-2})	Stand basal area. For 2LHM only.	

1380

Table 2. Model versions and their calibration/optimization parameters.

Model version	Heat Mass represented	Number of canopy layers	Calibration parameters
1LnoHM	No	1	k_{LAI}
1LHM	Yes	1	k_{LAI}
2LHM	Yes	2	k_{LAI} f_{LAI}
1LHM*	Yes	1	k_{LAI} HM_{can}
2LHM*	Yes	2	k_{LAI} f_{LAI} HM_{trunk}

Table 3. Model performance after calibration and optimization over 2003-2004. The calibration criterion CC is in bold. The * denotes versions where heat mass is optimized and not physically derived.

Model version	Calibration over 2003-2004											
	Bestfit parameter	Results over 2003-2004					Results over 2003-2007				
		RMSE LW	MB LW	RMSE SW	MB SW	CC	RMSE LW	MB LW	RMSE SW	MB SW	CC
1LnoHM	k_{LAI} =0.75	14.1	-3.5	9.4	0.3	27.3	17.5	-9.5	9.1	1.4	37.5
1LHM	k_{LAI} =0.75	11.5	-2.5	9.4	0.3	23.6	14.5	-10.6	9.2	1.8	36.0
2LHM	f_{LAI} =0.5 k_{LAI} =0.75	8.3	-0.7	9.3	0.2	18.4	9.6	-6.7	9.1	1.6	27.0
1LHM*	k_{LAI} =0.8 HM_{can}=90	*8.7*	*-0.7*	*9.4*	*-0.8*	*19.3*					
2LHM*	k_{LAI} =.75 f_{LAI} =0.6 HM_{trunk}=60	*7.9*	*0.1*	*9.3*	*0.2*	*17.5*					

Table 4. Model performance after calibration over 2003-2007.

Model version	Calibration over 2003-2007											
	Best fit parameter	Results over 2003-2004					Results over 2003-2007				
		RMSE LW	MB LW	RMSE SW	MB SW	CC	RMSE LW	MB LW	RMSE SW	MB SW	CC
1LnoHM	k_{LAI} =0.75	13.4	-2.4	9.4	-0.9	26.2	17.2	-9.1	9.0	0.2	27.3
1LHM	k_{LAI} =0.85	11.4	-1.7	9.8	-1.8	24.8	14.2	-9.8	9.2	-0.5	33.8
2LHM	k_{LAI} =0.85 f_{LAI} =0.5	8.2	0.3	9.8	-1.8	18.7	9.1	-5.8	9.2	-0.6	24.8

Table 5. Statistics of model evaluation at Norunda. *"corr"* is the correlation coefficient. The mean modelled and observed biomass (and biomass+air) heat fluxes are null over a period between two equal thermal states.

Field data Model version	Trunk temperature at 1.5 m (K)			Biomass heat flux (W m-2)		Biomass + air heat storage flux (W m-2)	
	MB	RMSE	corr	RMSE	corr	RMSE	corr
1LnoHM	-0.41	1.7	0.88	16.3	0.	24.2	0.
1LHM	-0.05	1.6	0.92	24.5	0.79	18.9	0.86
2LHM	0.05	1.1	0.96	15.7	0.88	11.3	0.92

Figures captions

1395   **Figure 1.** Radiative and turbulent fluxes in the 2-layer canopy module. <mark>Ellipses</mark> feature radiation sources, dotted lines indicate radiation absorption within the layer with the indicated absorption factor; albedos at the border between layers are underlined. For turbulent fluxes, arrows denote aerodynamic resistance.

1400   **Figure 2.** Typical event when snow-on-sensor is suspected. a. observed and modelled $LW\downarrow_{BC.}$ b. observed precipitation record.
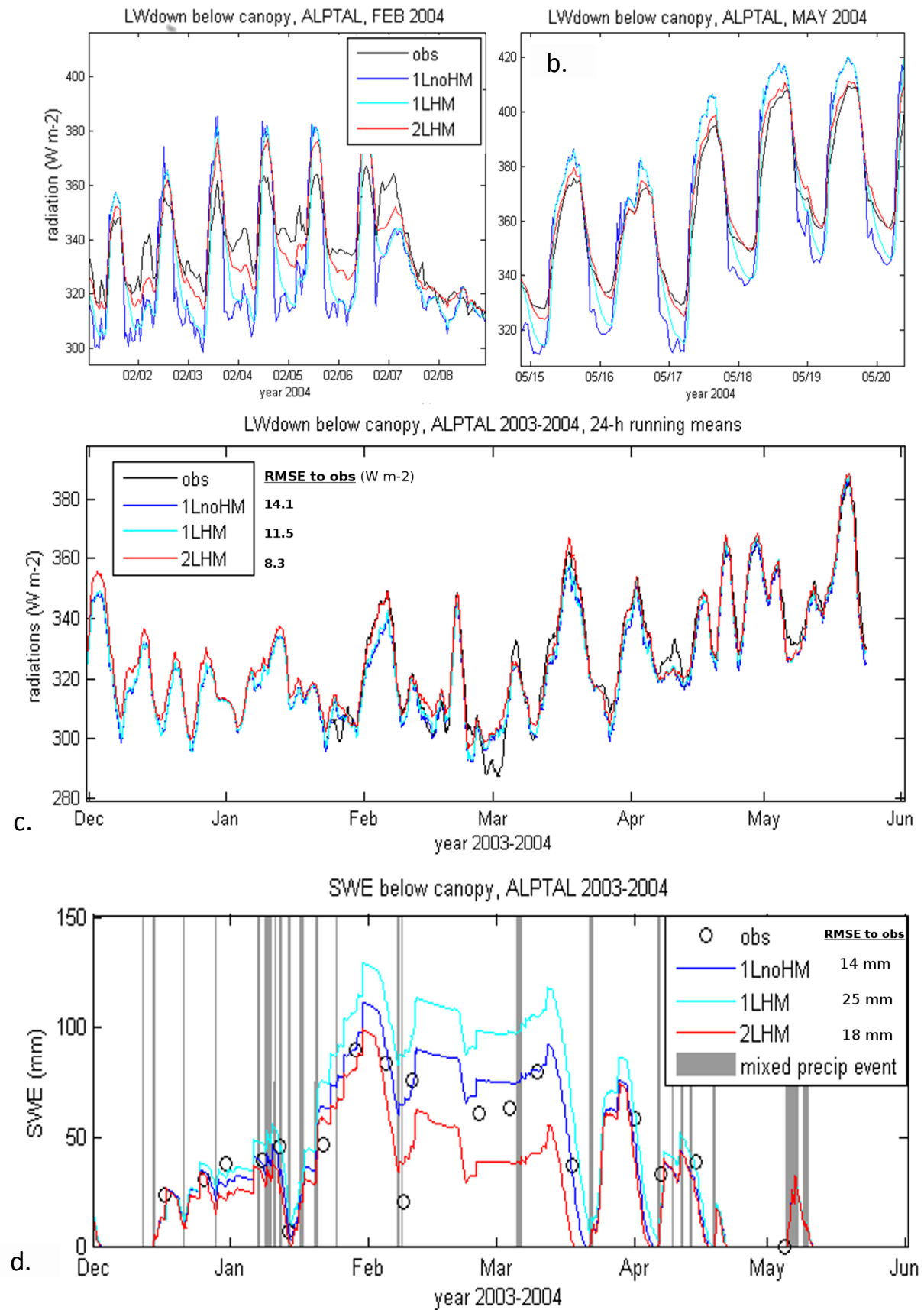
1405

Figure 4. Sub-canopy SWE at Alptal over 2004-2007.

1410   **Figure 5.** Comparison between observed Pine trunk temperature at 1.5 m height, 1 cm deep into the trunk, and modelled canopy temperatures: bulk canopy temperature for 1LnoHM and 1LHM, lowermost canopy-layer temperature for 2LHM.

Figure 6. Comparison between biomass (and biomass+air) storage fluxes inferred from observations
1415   (obs) and biomass fluxes modelled by the different SNOWPACK versions (model) at Norunda.

Figure 7. Sensitivity of model performance over 2003-2007 (with k_{LAI} =0.85) to f_{LAI} .The MB and RMSE are for the variables SW$\downarrow_{BC}$ (SW in the legend) and LW$\downarrow_{BC}$ (LW in the legend).